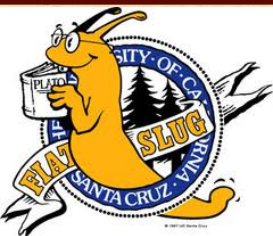


# *Recent progress in silicon sensor development for ATLAS tracking detector upgrade*

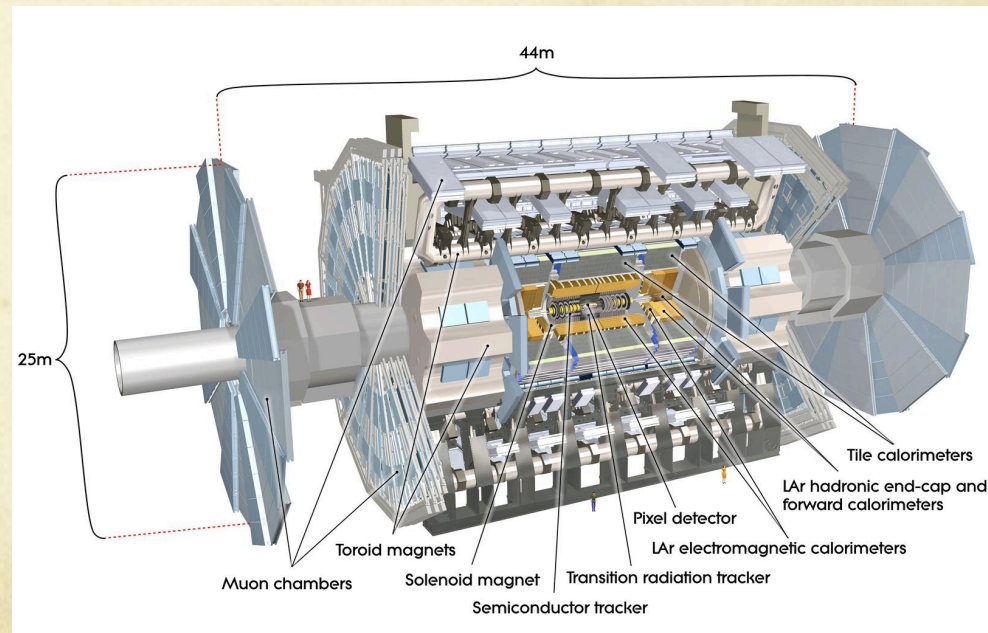
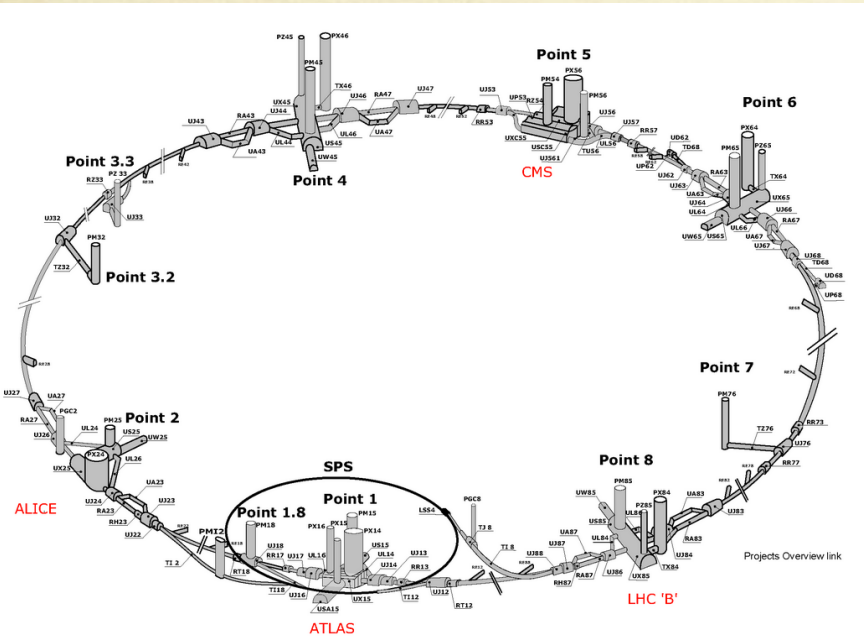
**Zhijun Liang\***

*University of California, Santa Cruz*



# Outline

- Current status of the ATLAS detector
  - Overview of the ATLAS electroweak physics results
- ATLAS upgrades
  - Upgrade physics motivation
  - Strip detector upgrade
  - Sensor research and development



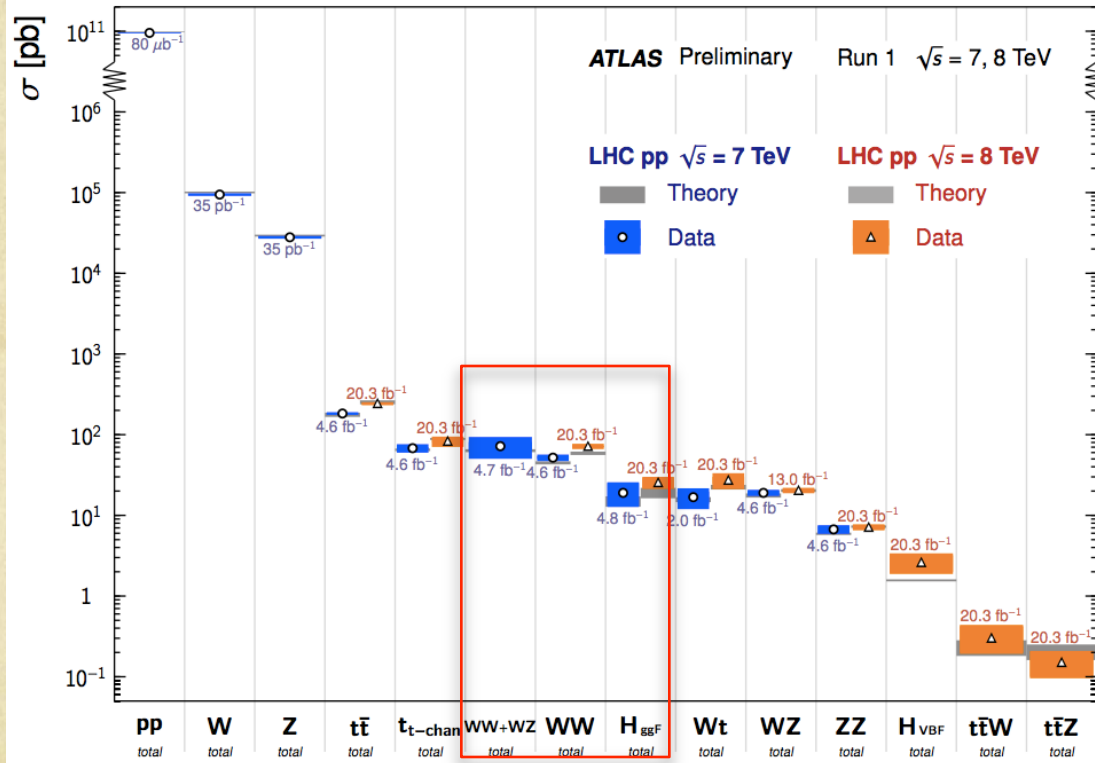


# Overview ATLAS Standard models(SM) measurements

- This talk focuses on SM electroweak measurements

Standard Model Total Production Cross Section Measurements

Status: July 2014

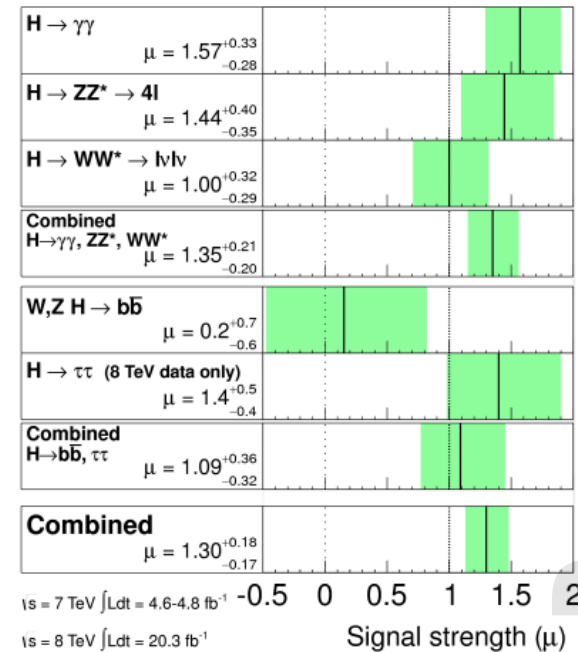


ATLAS Preliminary

$m_H = 125.5 \text{ GeV}$

Total uncertainty

■  $\pm 1\sigma$  on  $\mu$



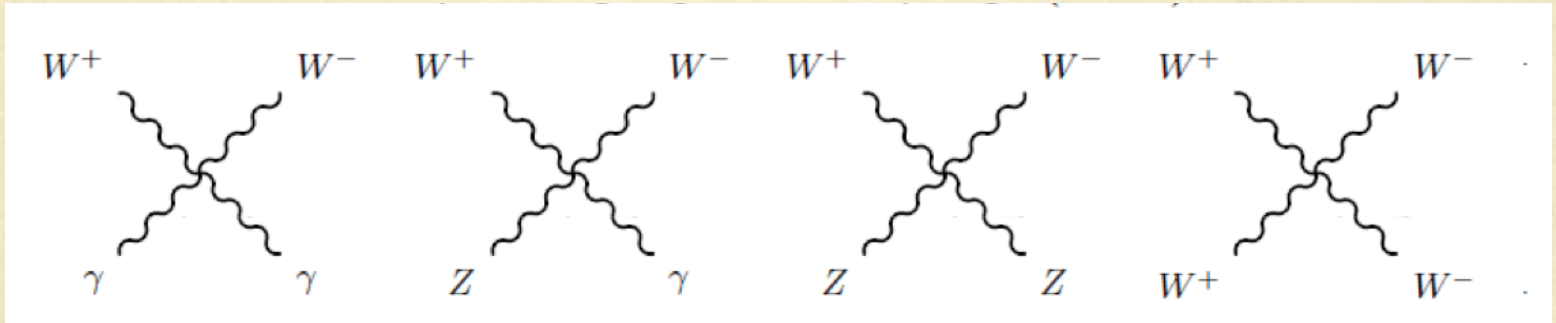
# Motivation for high luminosity running

- Current LHC project is designed to collect  $300\text{fb}^{-1}$  data
- The motivation of High luminosity upgrade (HL-LHC) for SM physics (up to  $3000\text{fb}^{-1}$ )
  - More precise measurement of the Higgs boson properties
    - All Higgs coupling , especially H couplings to fermions
  - More precise measurement of gauge boson self-coupling
    - Study the dynamic of electroweak symmetry breaking (EWSB)

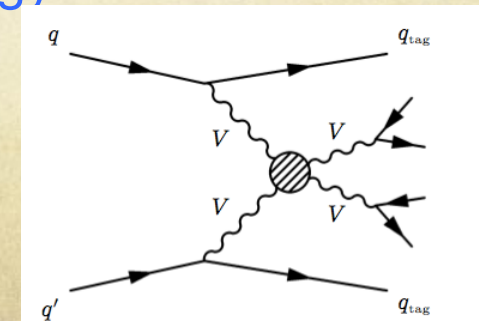
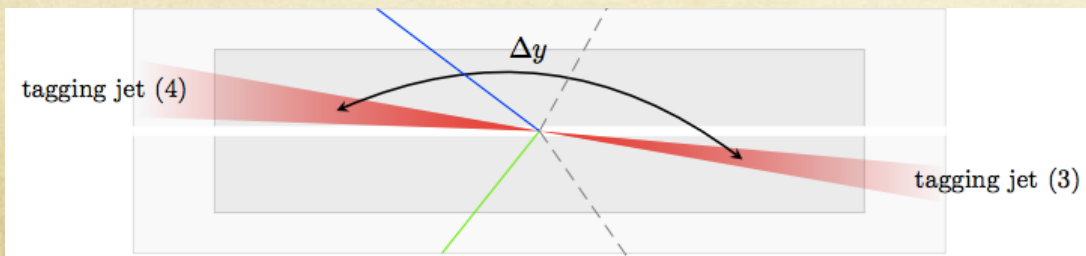


# Quartic Gauge Boson Couplings and vector boson scattering (VBS)

- The Higgs mechanism  $\neq$  a Higgs boson !
- Reminder of **Quartic Gauge Boson Couplings (QGCs)**
  - SM model predicts gauge boson self coupling
  - Four gauge boson vertex:



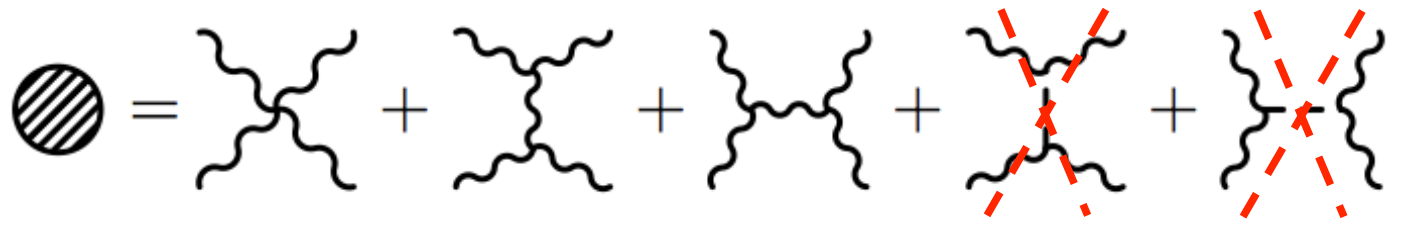
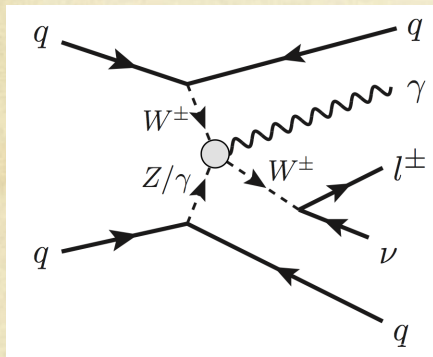
- Vector boson scattering (VBS) is one of the process to study QGCs.
- Diboson + two forward jets in event topology



# Introduction to $W/Z\gamma$ +dijet VBS

- $W\gamma$ +dijet VBS : photon+ lepton+ $E_T^{\text{miss}}$ + dijet
  - Sensitive to QGCs in  $WW\gamma\gamma$ ,  $WWZ\gamma$  vertex
- $Z\gamma$ +dijet VBS : photon+ two opposite charge leptons + dijet
  - Sensitive to QGCs in  $WWZ\gamma$  vertex
  - No contamination from aTGCs

## $W\gamma$ +dijet VBS



QGCs

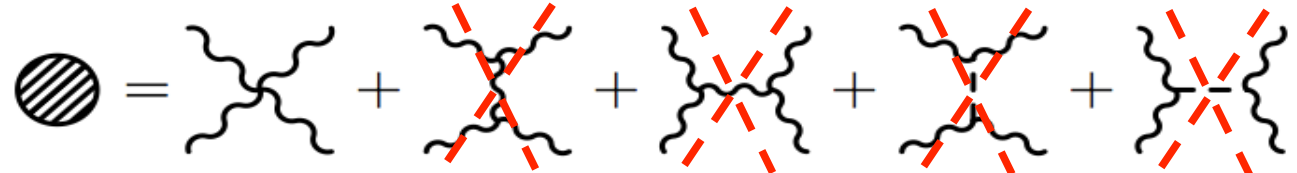
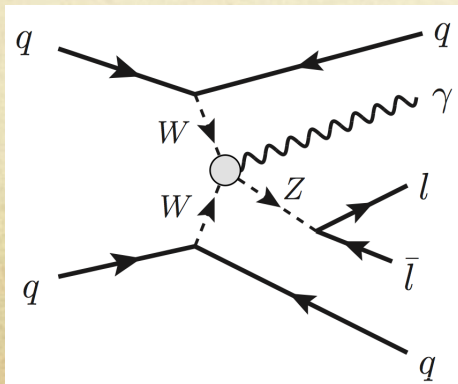
TGCs  
T channel

TGCs  
S channel

Higgs  
t channel

Higgs  
S channel

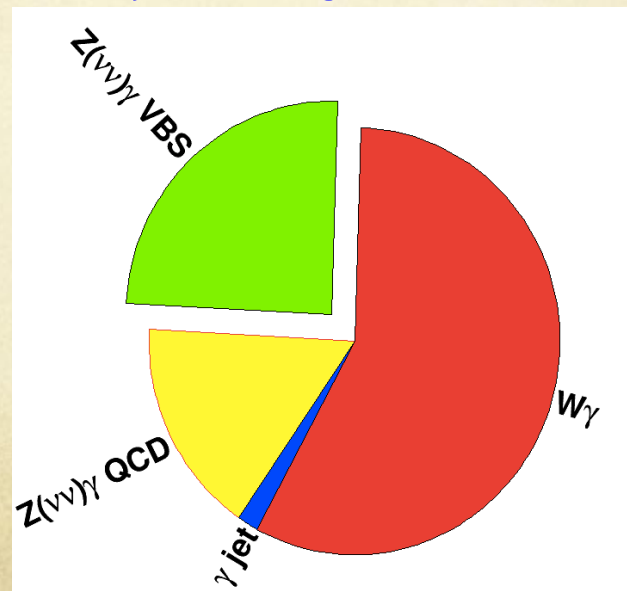
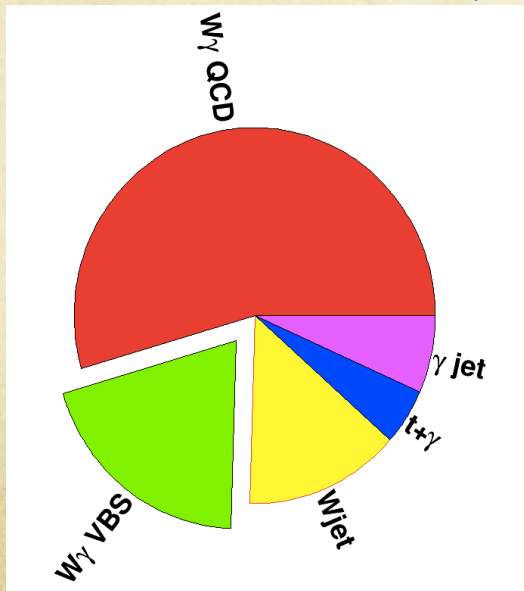
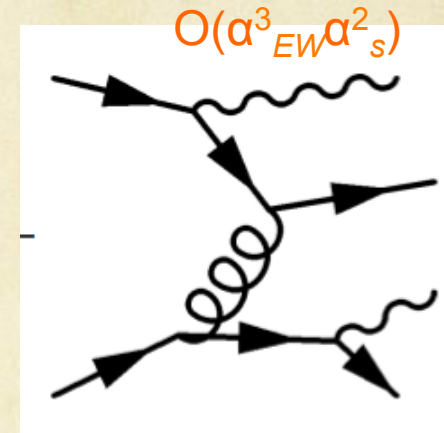
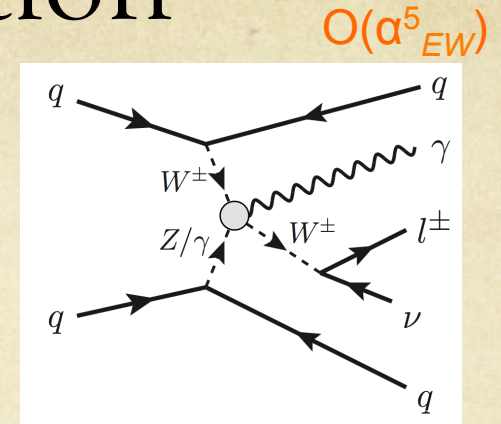
## $Z\gamma$ +dijet VBS





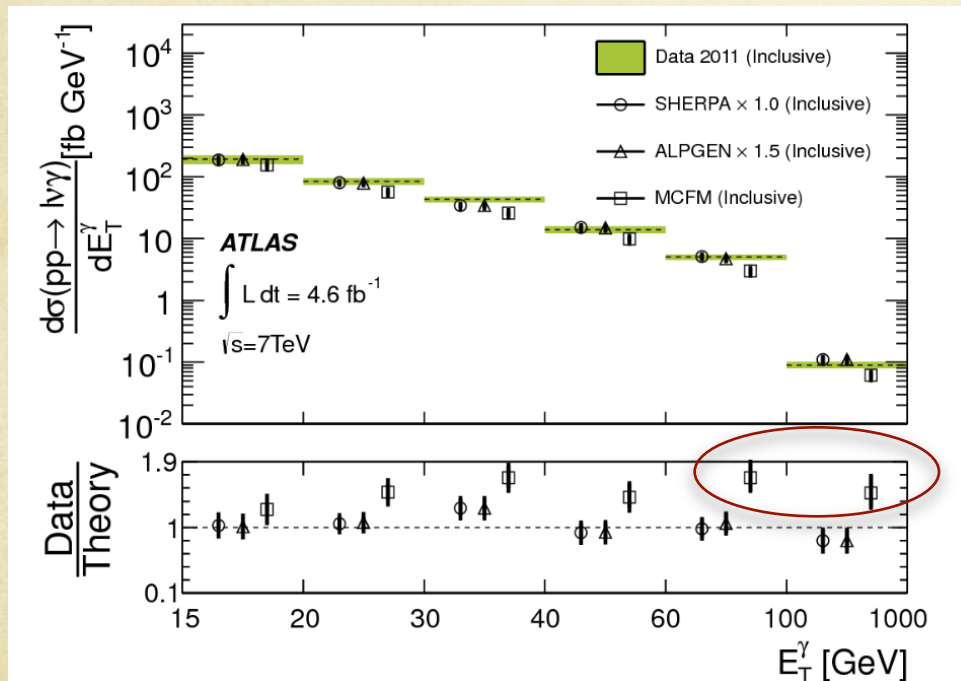
# Background composition

- $W(l\nu) \gamma$  +dijet VBS analysis
  - $W(l\nu) \gamma$  +dijet QCD :  $O(\alpha_{EW}^3 \alpha_s^2)$   
 Jets from QCD coupling vertex
  - $W$ +jets: jets fake as photon
  - $\gamma$  +jets: jet fake as lepton
- $Z(\nu\nu) \gamma$  VBS analysis
  - $W(\tau \nu) \gamma$  +dijet VBS is major background



# $W\gamma$ ( $lv\gamma$ ) : photon $E_T$

- Unfolded Photon  $E_T$  spectrum compared to MCFM NLO predictions
  - Discrepancy in high  $E_T$  for inclusive measurement (without jet veto)
- Data compared to Sherpa/Alpgen predictions
  - Very good agreement in event kinematics
  - Scale up the Alpgen predictions by a factor of 1.5 to match data.



Phys. Rev. D 87, 112003 (2013)

## • $W\gamma$ ( $lv\gamma$ ) Selection

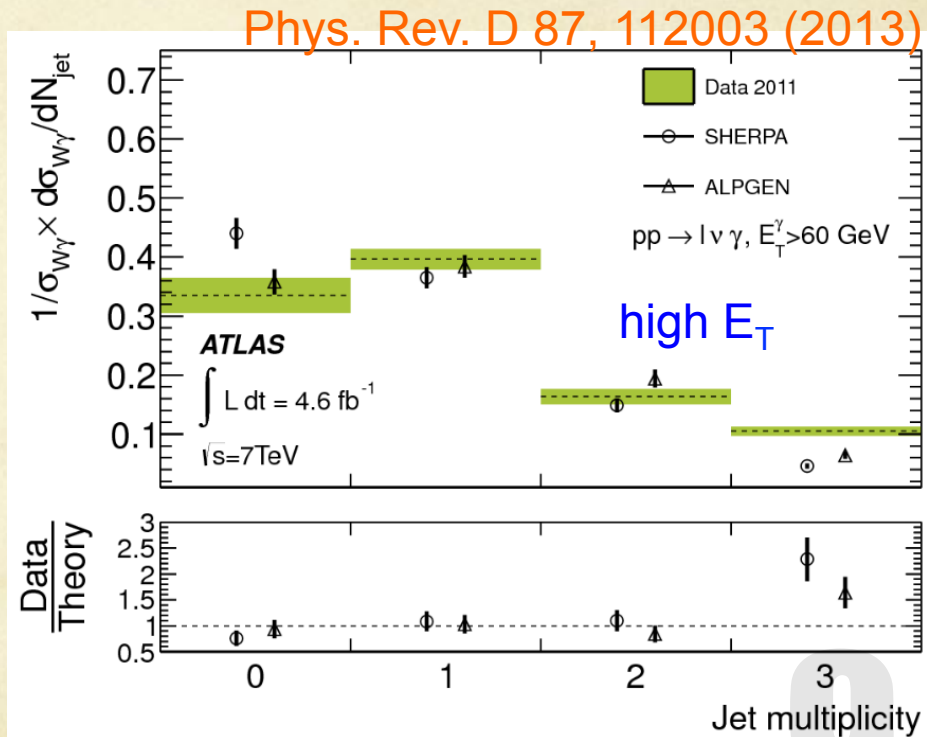
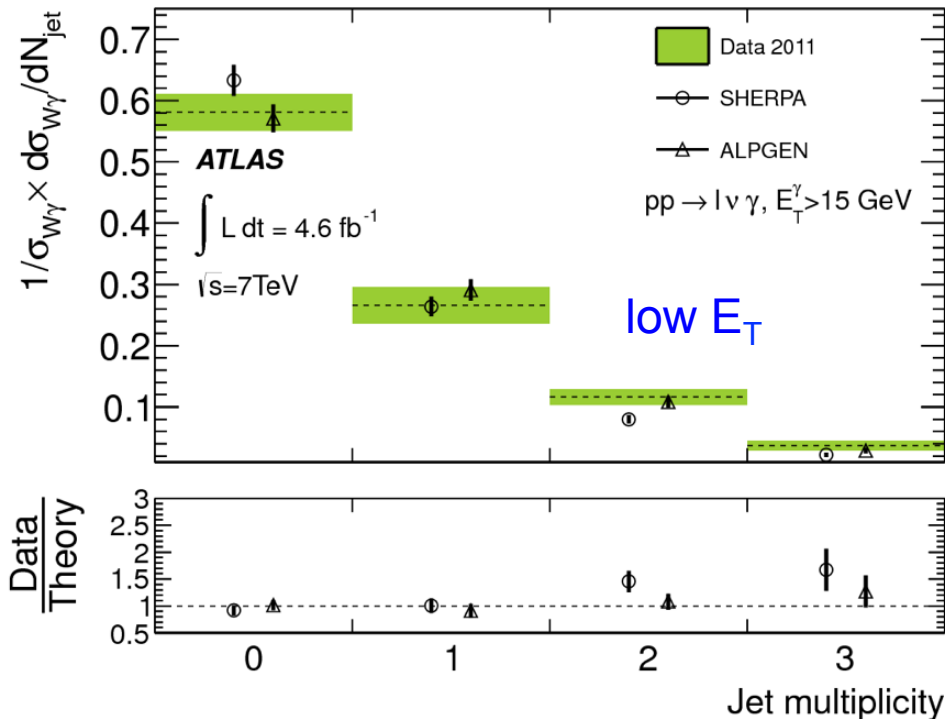
- One lepton with  $p_T > 25 \text{ GeV}$
- $E_T^{\text{miss}} > 35 \text{ GeV}$
- One photon with  $p_T > 15 \text{ GeV}$

Sherpa : Matrix element calculation for  $W\gamma+0/1/2/3$  partons  
Alpgen: Matrix element calculation for  $W\gamma+0/1/2/3/4/5$  partons



# $W \gamma$ ( $l \nu \gamma$ ): Jet multiplicity

- Jet multiplicity depends strongly on photon  $E_T$  threshold.
  - Dominant contribution from 0jet bin in low  $E_T$  region
  - Dominant contribution from 1jet bin in high  $E_T$  region
  - Contributions from 2jet or 3jet bins are not negligible

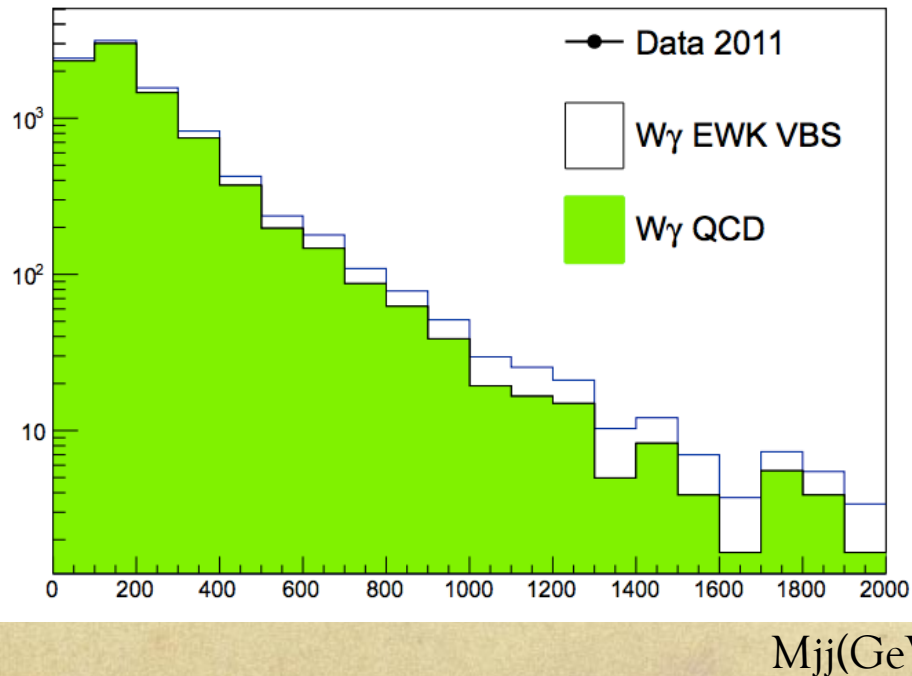


Sherpa :Matrix element calculation for  $W\gamma+0/1/2/3$  partons  
 Alpgen: Matrix element calculation for  $W\gamma+0/1/2/3/4/5$  partons

# Signal significance @ 8TeV

Number of expected candidates @8TeV	$W_{\gamma jj}$ EWK	$W_{\gamma jj}$ QCD	$S/\sqrt{B}$
After VBS selection	120	450	$\sim 5$

Generator study



## • $W_{\gamma}$ ( $l\nu_{\gamma}$ ) Selection

- ☐ One lepton with  $p_T > 25 \text{ GeV}$
- ☐  $E_{T}^{\text{miss}} > 35 \text{ GeV}$
- ☐ One photon with  $p_T > 15 \text{ GeV}$

After VBS selection

$M(jj) > 500 \text{ GeV}$ ,  $|\Delta Y(jj)| > 2.4$



# aQGC sensitivity

- Anomalous QGCs (aQGCs) coupling will change the events kinematics
- Eboli's EFT dimension 8 model is used to model aQGCs scenario
- $W\gamma jj$ 
  - Sensitive to WWAZ, WWAA coupling
- $Z\gamma jj$ 
  - Sensitive to WWAZ, ZZAA, ZAAA coupling

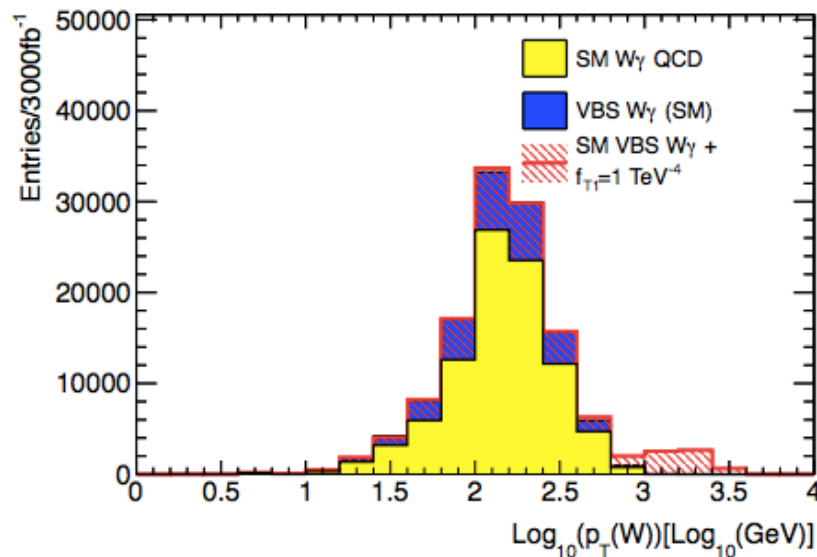
	WWWW	WWZZ	ZZZZ	WWAZ	WWAA	ZZZA	ZZAA	ZAAA	AAAA
$\mathcal{L}_{S,0}, \mathcal{L}_{S,1}$	X	X	X	O	O	O	O	O	O
$\mathcal{L}_{M,0}, \mathcal{L}_{M,1}, \mathcal{L}_{M,6}, \mathcal{L}_{M,7}$	X	X	X	X	X	X	X	O	O
$\mathcal{L}_{M,2}, \mathcal{L}_{M,3}, \mathcal{L}_{M,4}, \mathcal{L}_{M,5}$	O	X	X	X	X	X	X	O	O
$\mathcal{L}_{T,0}, \mathcal{L}_{T,1}, \mathcal{L}_{T,2}$	X	X	X	X	X	X	X	X	X
$\mathcal{L}_{T,5}, \mathcal{L}_{T,6}, \mathcal{L}_{T,7}$	O	X	X	X	X	X	X	X	X
$\mathcal{L}_{T,9}, \mathcal{L}_{T,9}$	O	O	X	O	O	X	X	X	X

# aQGCs sensitivity

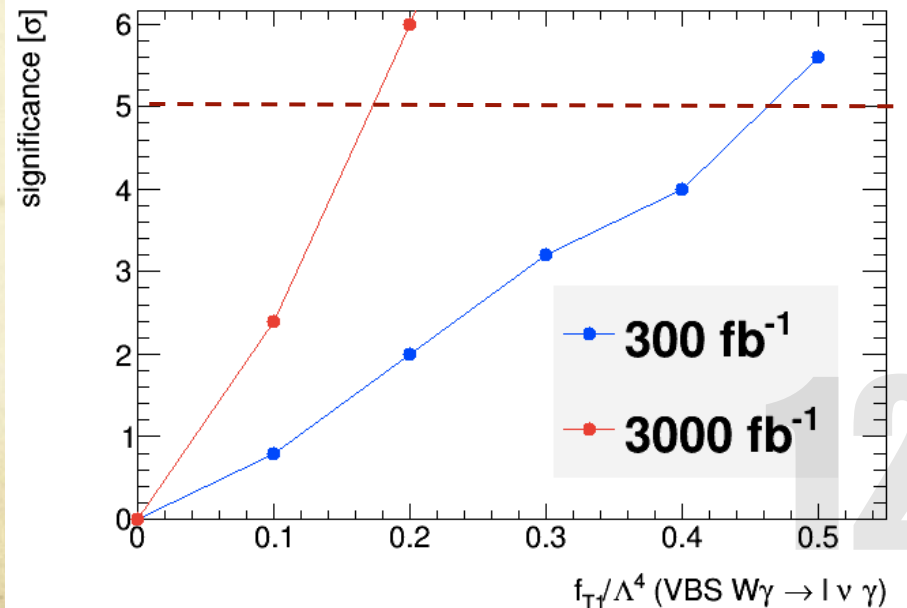
## LHC Vs HL-LHC

- The transverse momentum of the  $W$  boson is sensitive to aQGCs
- aQGCs sensitivity Improve by a factor of 3 using HL-LHC

Generator study



Generator study





# Another case for upgrade physics

## VBF $H + \gamma$

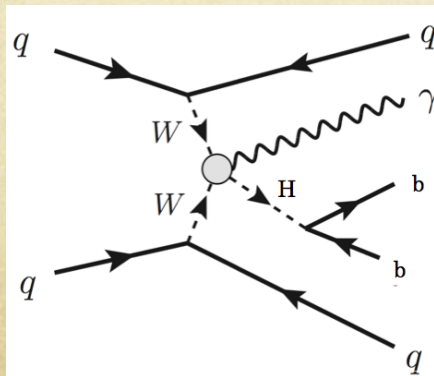
### Motivation

- $H \rightarrow b\bar{b}$  coupling has not been confirmed in experiment
- VBF Higgs production mechanism has not been confirmed

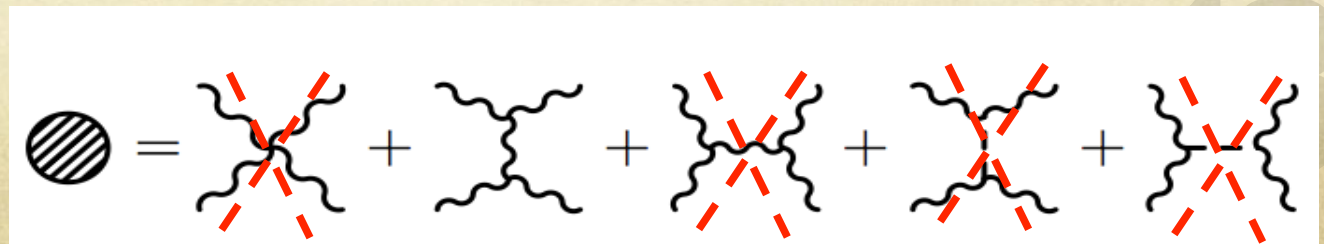
### Gluon fusion $H \rightarrow b\bar{b}$ and VBF $H(b\bar{b})$

- Large QCD background

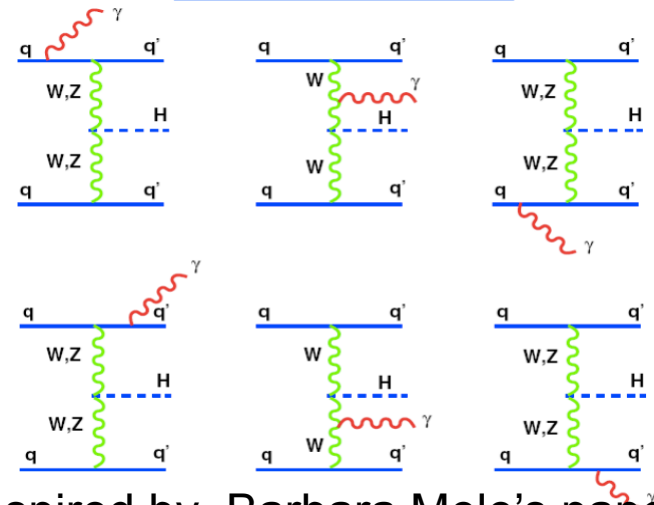
### VBF $H(b\bar{b}) + \gamma$



$H(b\bar{b})\gamma + \text{dijet VBF}$



$qq \rightarrow qq H + \gamma$



Inspired by Barbara Mele's paper  
<http://arxiv.org/abs/hep-ph/0702119>

# Major Background process

## VBF $H^+ \gamma$

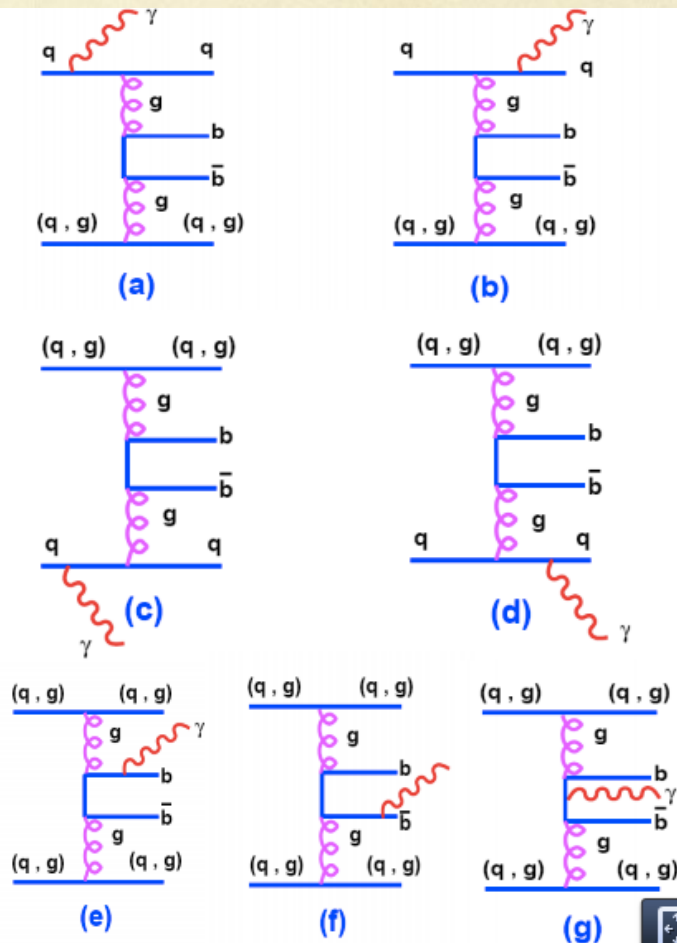
Inspired by Barbara Mele's paper  
<http://arxiv.org/abs/hep-ph/0702119>

- QCD  $bbjj + \gamma$  production

**bckg is less active by  
 requiring a central photon**

**dynamical effect:**  
**destructive interference**  
 for gamma at large angles  
 a) + b) and c) + d)

**dominant effect, but  
 suppressed by the b-quark  
 electric charge**



# VBF $H^+ \gamma$ : LHC Vs HL-LHC

Reco level (Generator study)	13TeV (300fb-1)	13TeV (3000fb-1)
N(signal)	80	800
N(BG)	556	5560
S/sqrt(B)	3.4	5.9

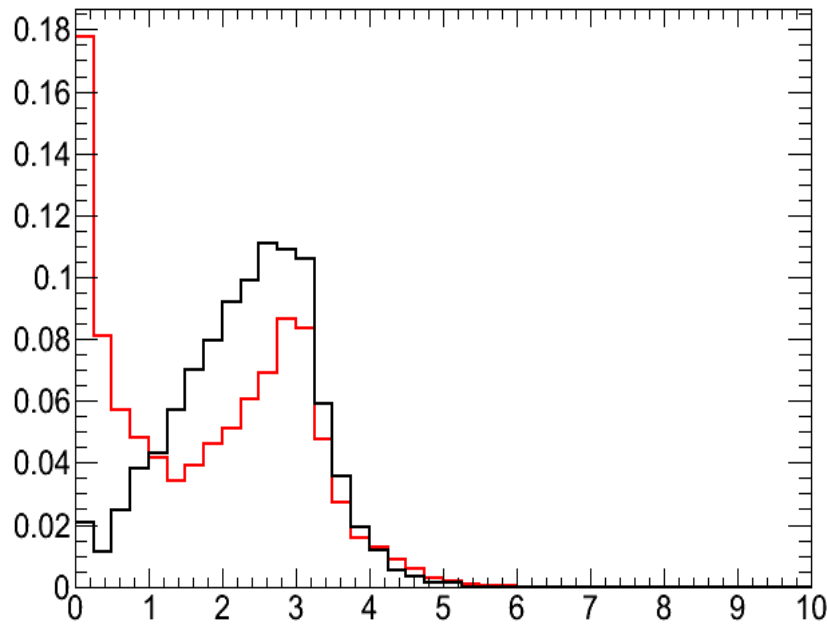
Selection cuts:

VBF dijet  $M_{jj} > 800 \text{ GeV}$

Leading jet  $p_T > 80 \text{ GeV}$ , other jets  
 $p_T > 30 \text{ GeV}$

$110 \text{ GeV} < M(bb) < 140 \text{ GeV}$

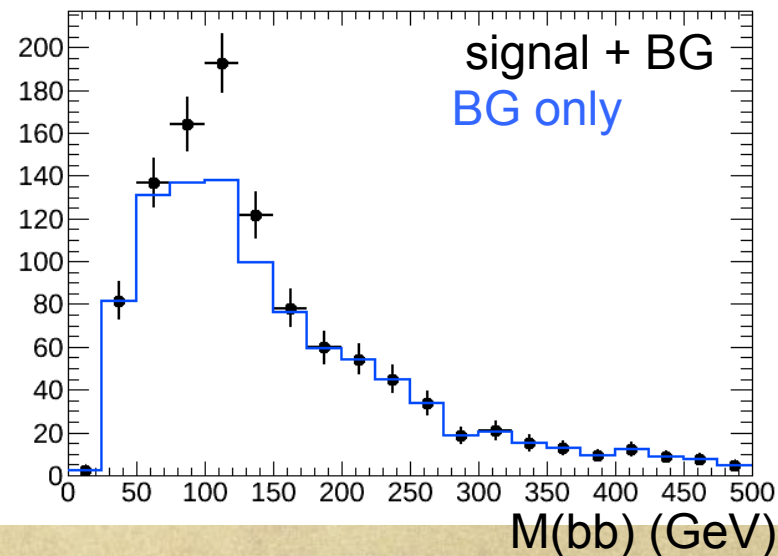
$DR(bjets; \text{photon}) > 1.2$



$DR(\gamma; bjets)$

MC generator study

13TeV (300 fb-1)

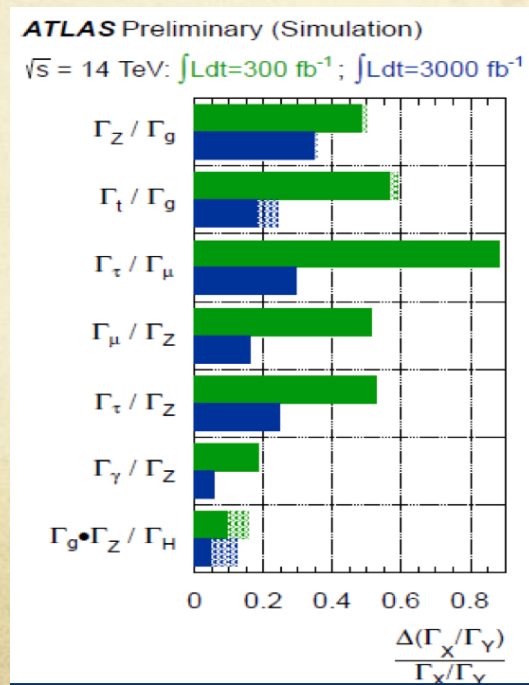


$M(bb)$  (GeV)



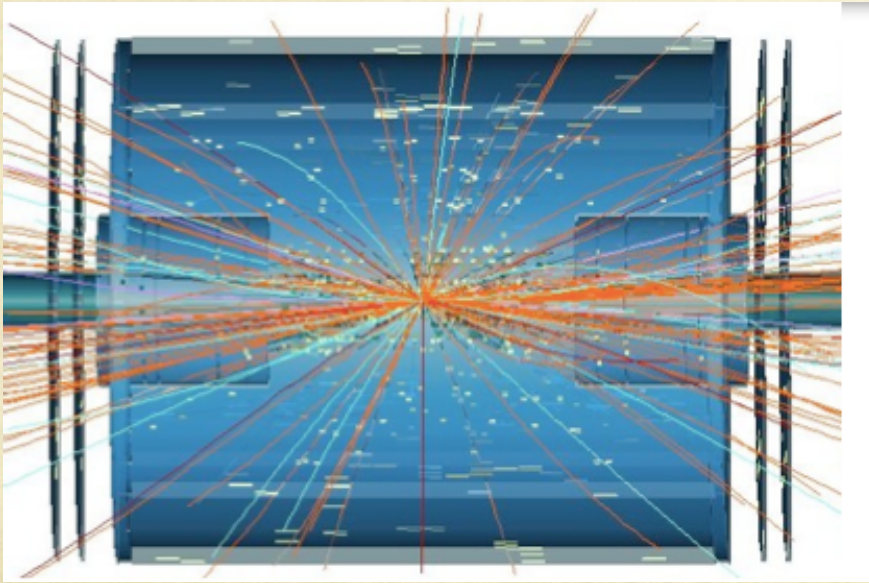
# why we need HL-LHC

- gauge boson self-coupling
  - aQGCs sensitivity Improve by a factor of 3 using HL-LHC
- VBF H+ $\gamma$ 
  - Signal significance goes from 3.4 (300fb<sup>-1</sup>) to 5.9 (3000fb<sup>-1</sup>)
- Other motivations in Higgs coupling measurements

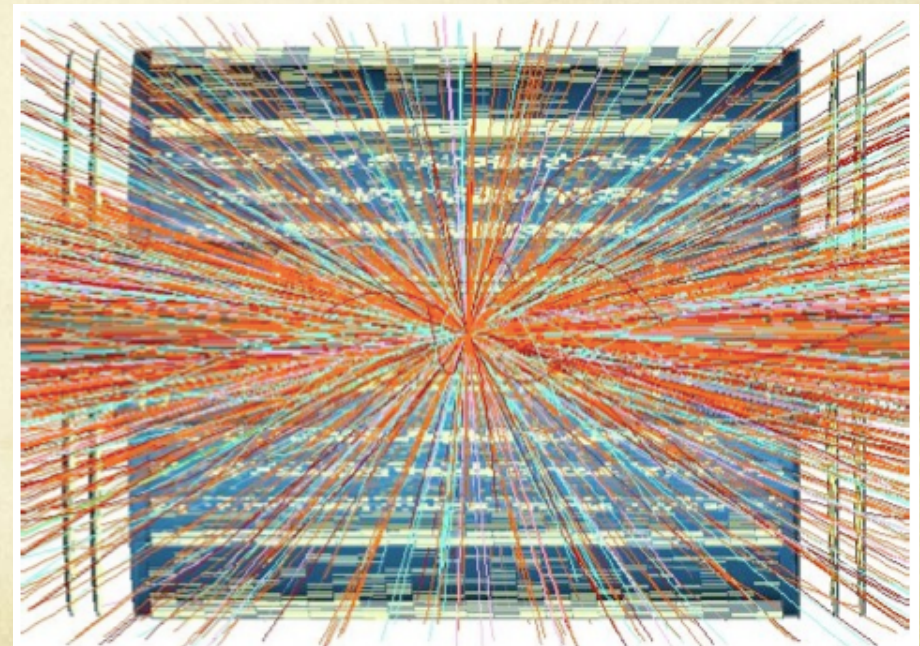


# Why to upgrade ATLAS detector

- To keep ATLAS running in HL-LHC requires tracker replacements
- Major difficulty in new tracker design
  - 10 times higher dose
  - Much higher occupancy (200 collisions per beam crossing )



LHC

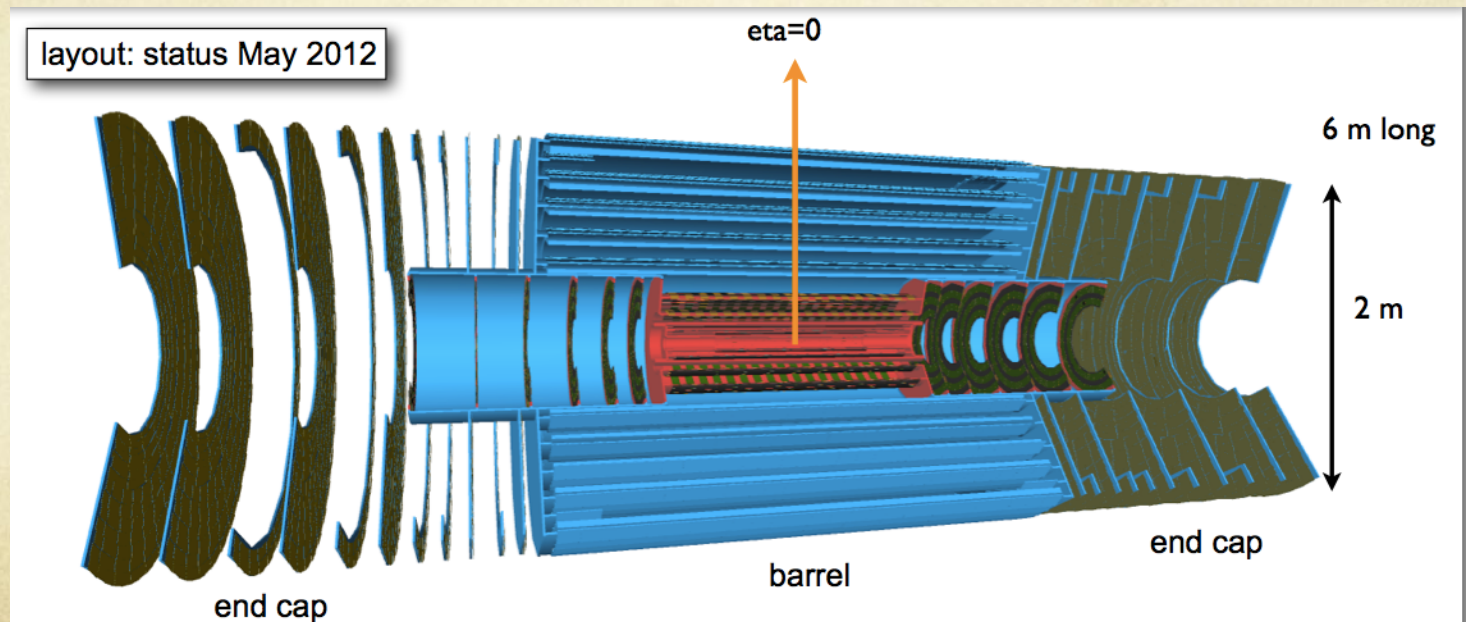


HL-LHC



# The new Tracker for ATLAS

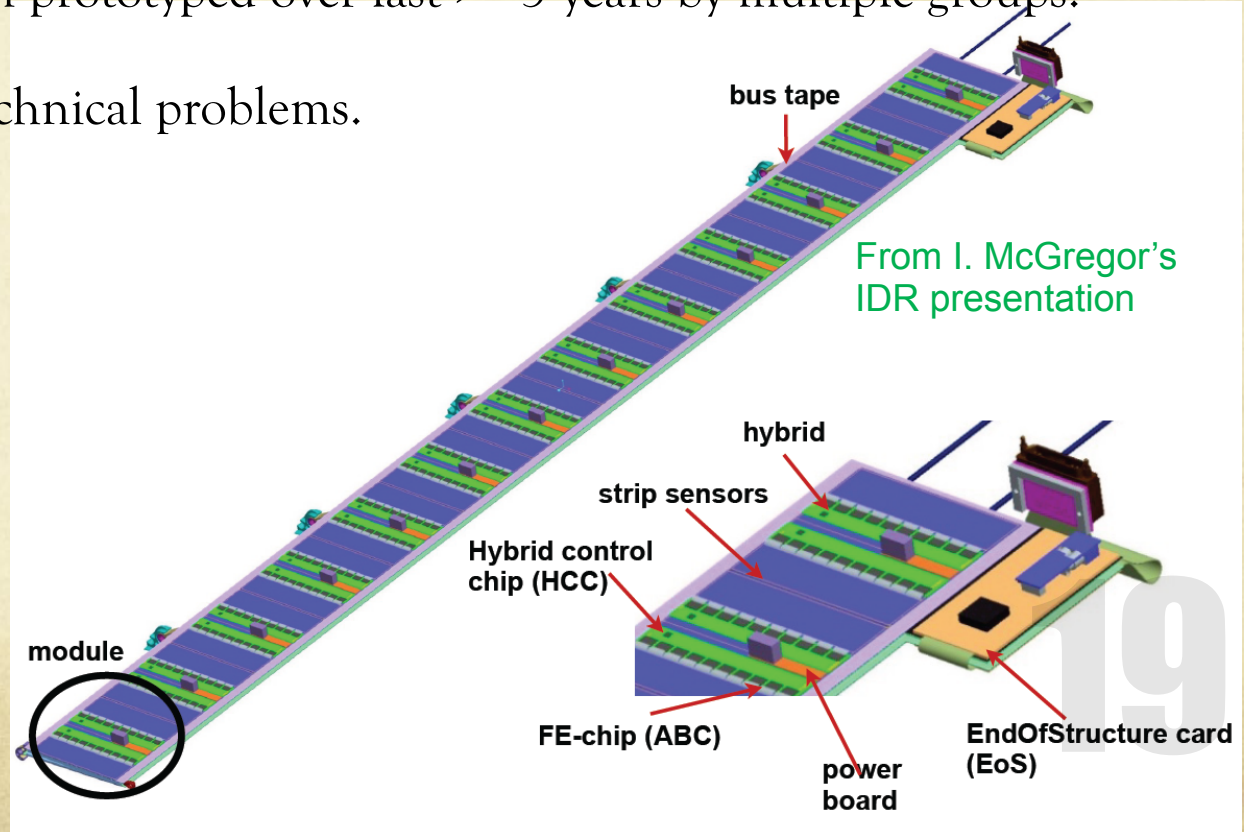
- Pixel: 4 barrel layer plus 6 disks on each side
  - 400 million pixels
- 5 double sided Strip layers plus 5 strip disks on each side
  - 60 million strips ( $\sim 200\text{m}^2$ )





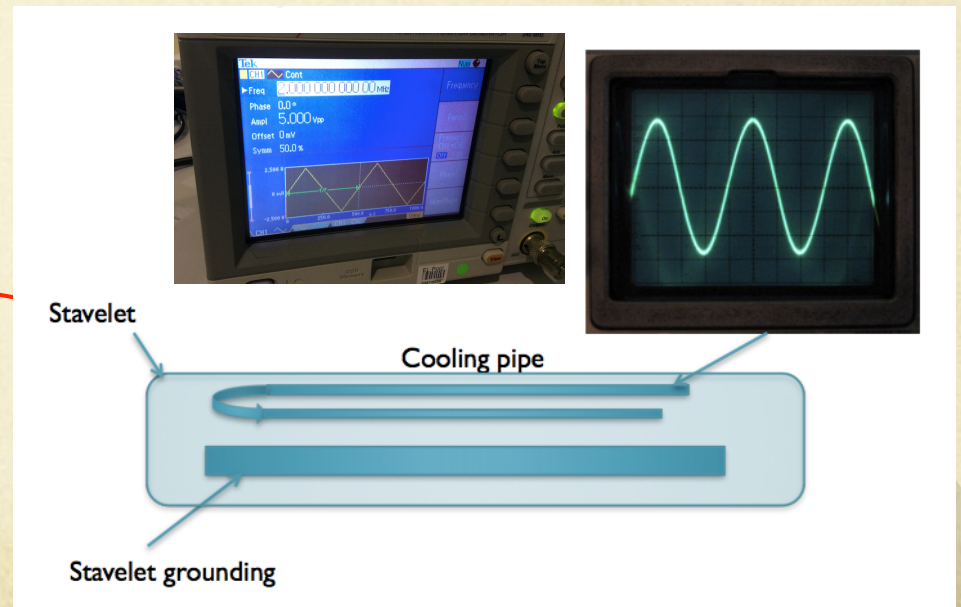
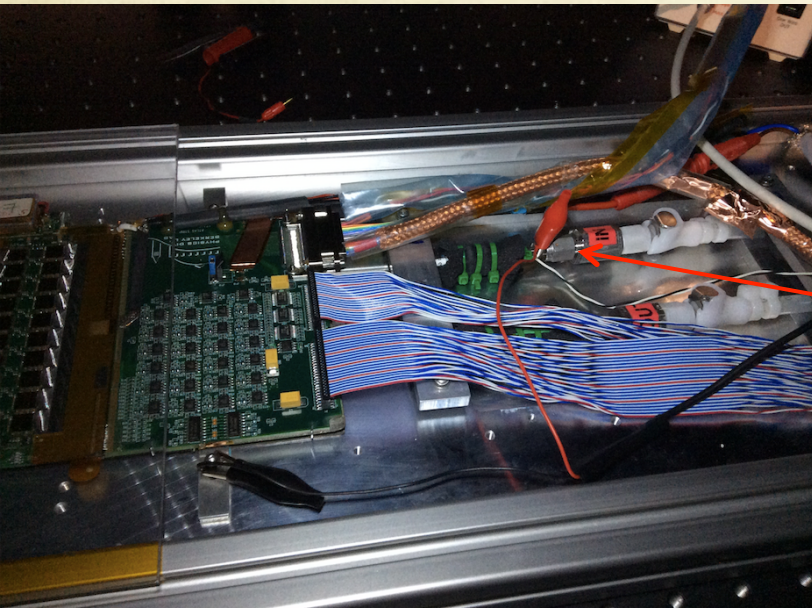
# Baseline ATLAS Strip Tracker

- The tracker ( $\sim 200 \text{ m}^2$ ) is composed of barrels/endcaps.
- Which are composed of staves/petals.
- Which are composed of modules.
- These objects have been prototyped over last  $\geq 3$  years by multiple groups.
- There are no serious technical problems.



# One example of Stave testing

- stave built as electrical test-bed
  - one example to use stave for Shielding and grounding test
  - Modules Noise measurements I made at CERN in building 180
  - Signal generator to generate noise
    - Injected from cooling pipe
    - Measure module input noise using 3 point gain tests.



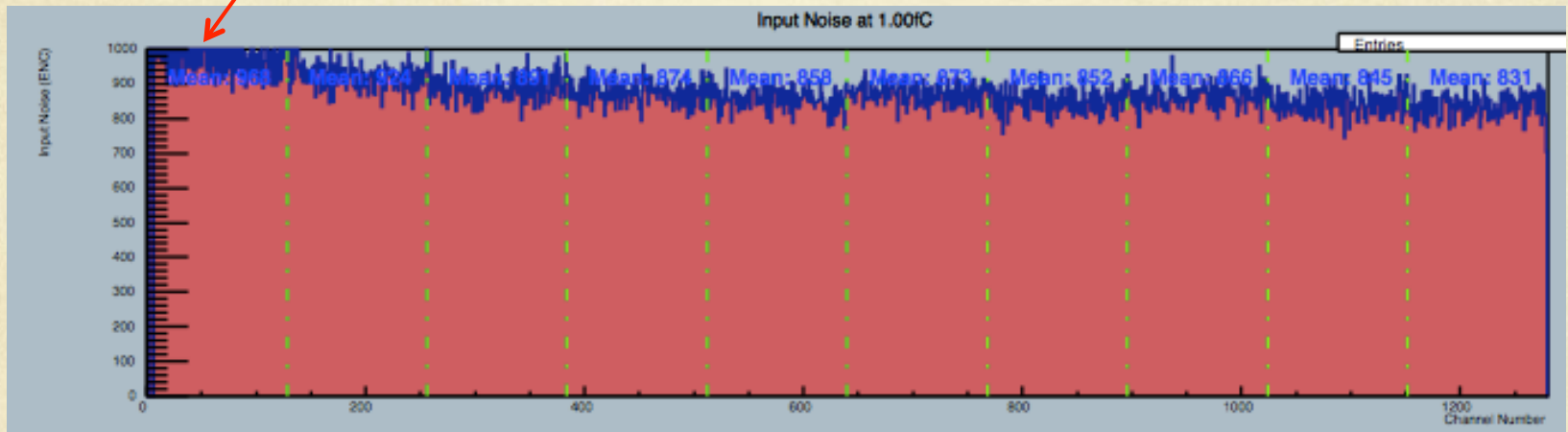


# Impact of noise in cooling pile

- There is quite big impact when given large injected noise
- Impact is bigger in first two chips (closer to cooling pipe)

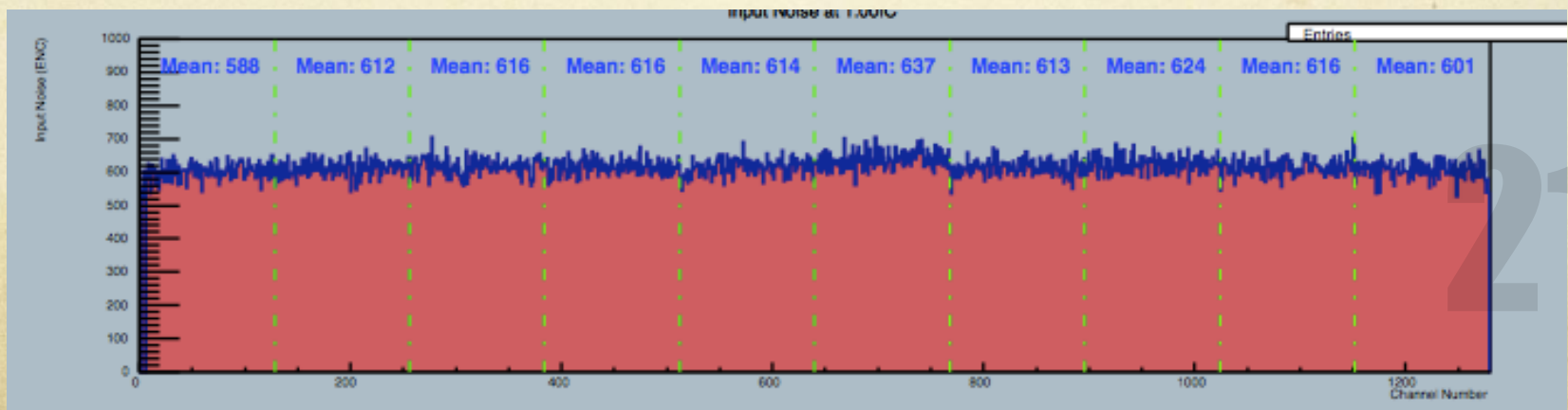
Input Noise (enc)

(injected external noise from cooling pipe on, 2Mz, 5Vpp)



Input Noise (enc) (injected noise off, normal case)

Channel

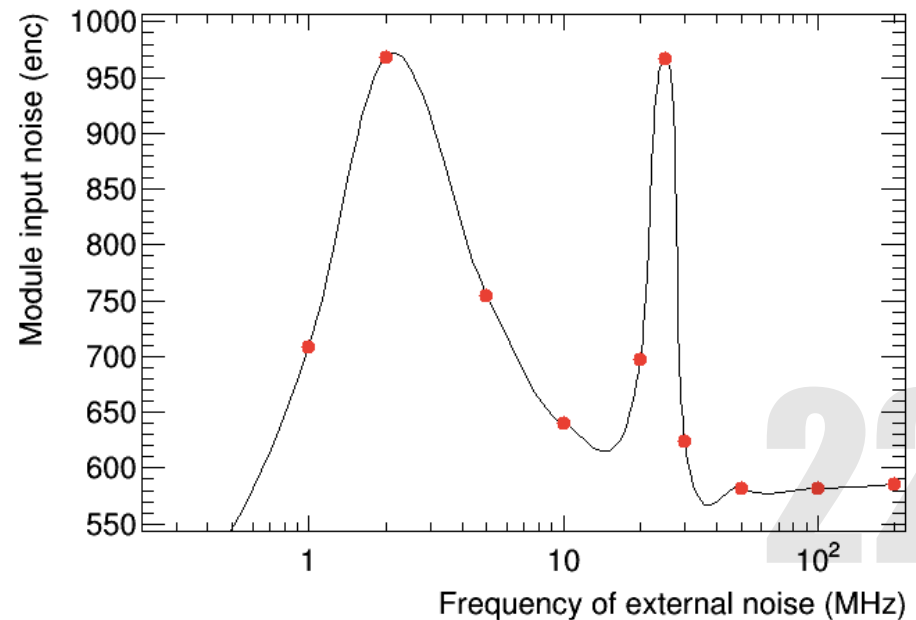
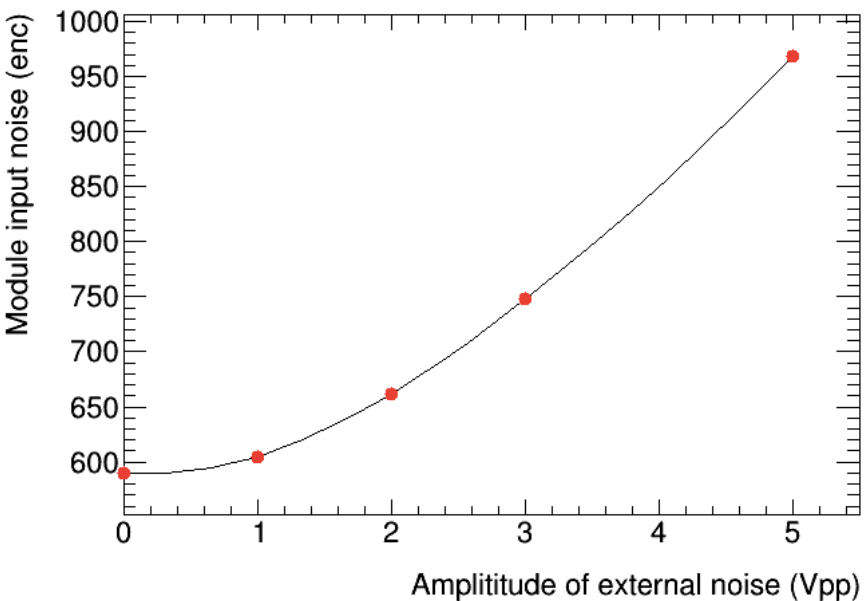




# Amplitude of external noises $V_s$

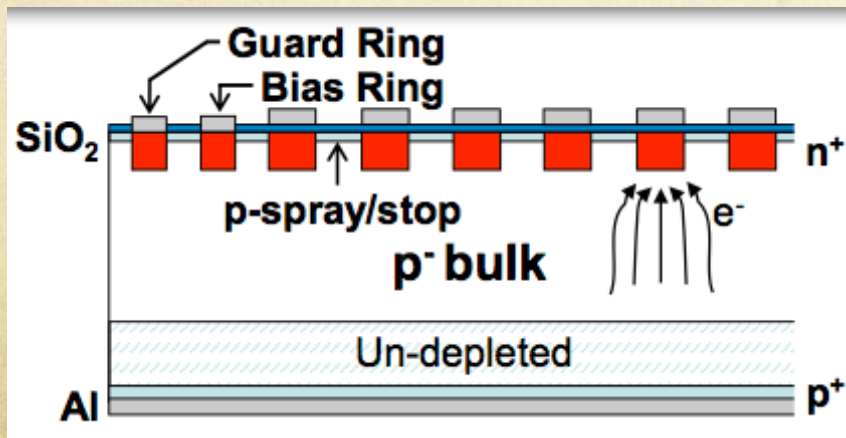
## Module Noise

- Module on a small stave (stavelet) is more sensitive to some certain frequency of noise.



# Radiation Hard Sensors

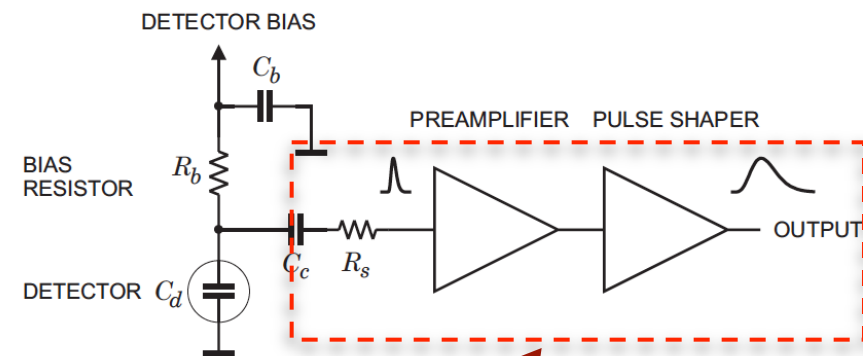
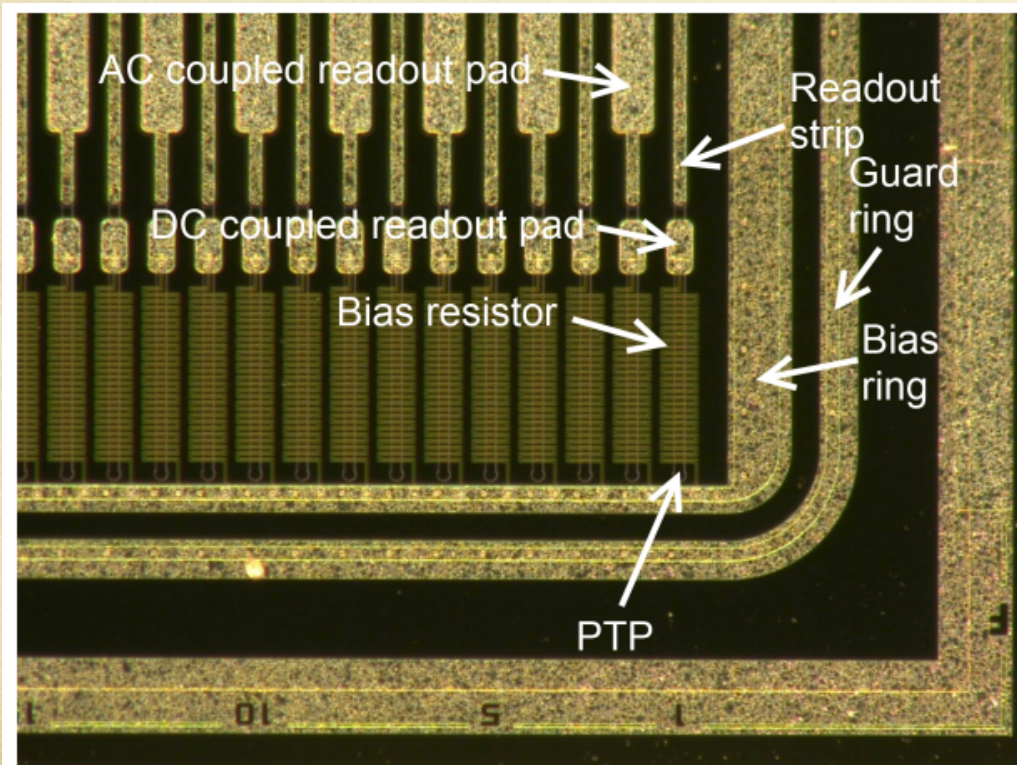
- Sensors: n in p single sided design, 98 x 98 mm, long & short strip designs, detailed design not yet finalized
- n<sup>+</sup>-strip in p-type substrate (n-in-p)
  - Collects electrons like current n-in-n pixels
  - Faster signal, reduced charge trapping
- The study of planar sensors are quite advanced
  - Lots of study have been done for radiation hardness
  - Full size sensor has been studied





# Sensor layout

- Bias ring is connected to ground.
- Bias resistor is designed for providing uniform HV
- AC coupling readout pad is wire bonded to readout chip



readout chip



# Radiation hardness study

- Samples

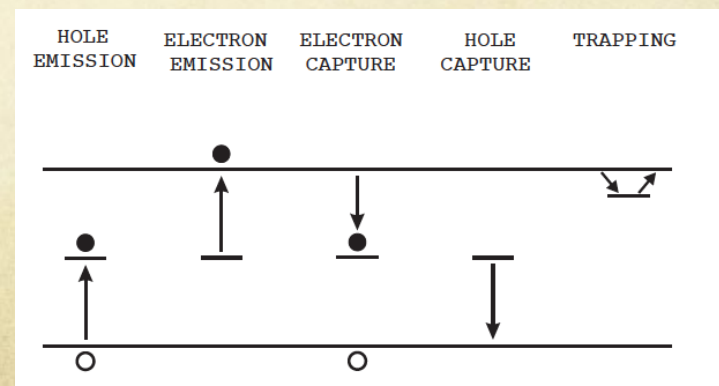
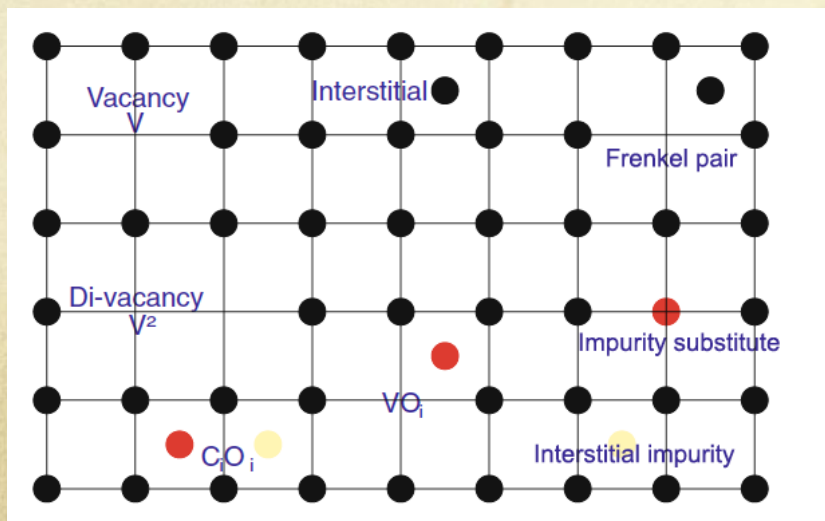
- ATLAS12A samples radiated with gamma at BNL

- Many Thanks to David Lynn

- 4 fluences : 10 Mrad , 3Mrad, 1Mrad , 300krad, 100krad

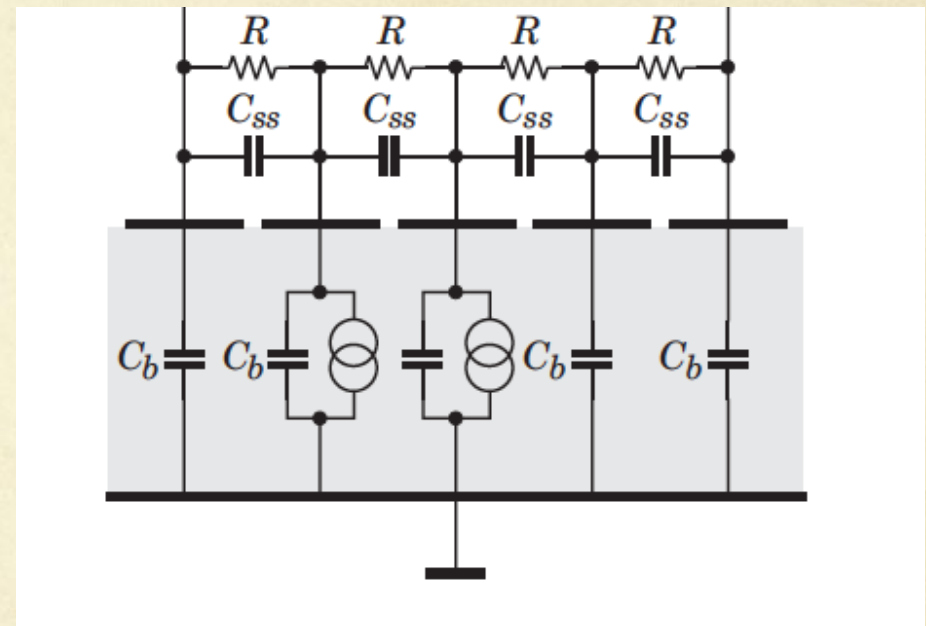
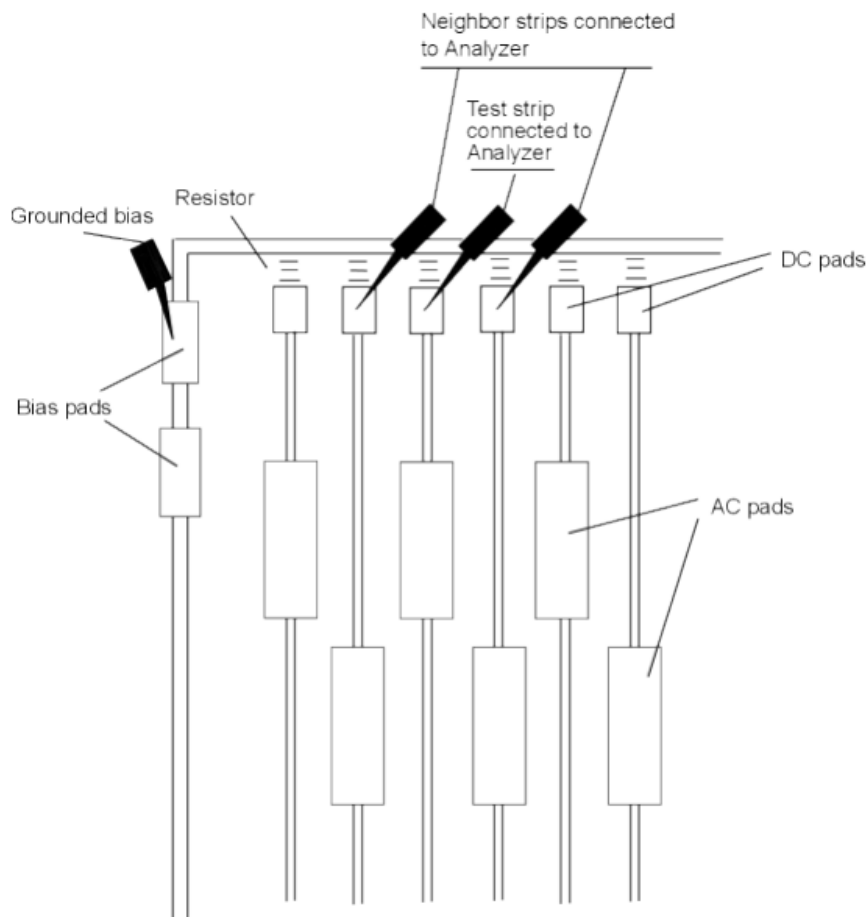
# Reminder of radiation damage

- What happen to Silicon sensor after bulk radiation damage:
  - Displacements in the silicon lattice
  - Creating intermediate state
    - Lead to higher leakage current
  - Defect state will capture the charge carriers
    - lead to lower charge collection efficiency
  - Lead to cross talk in signal readout
    - Lower isolation between two close-by strips or pixels
    - Higher inter-strip or inter-pixel capacitance



# Inter-strip resistance measurement

- ❑ Inter-strip resistance is the resistance between strips
- ❑ Radiation damage will reduce the inter-strip resistance
- ❑ Low Inter-strip resistance
  - ❑ Result in larger cross talk -> low position resolution



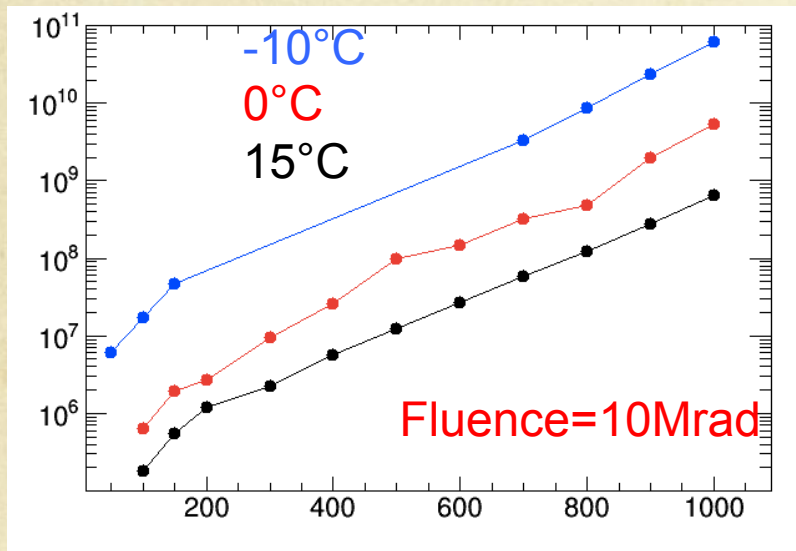
Measure nA current for G $\Omega$  level resistance  
Relative low S/N  
Do a careful job in grounding to reduce the noise



# Inter-strip resistance Vs temperature

- Higher resistance in low temperature
- Higher resistance with higher bias voltage.

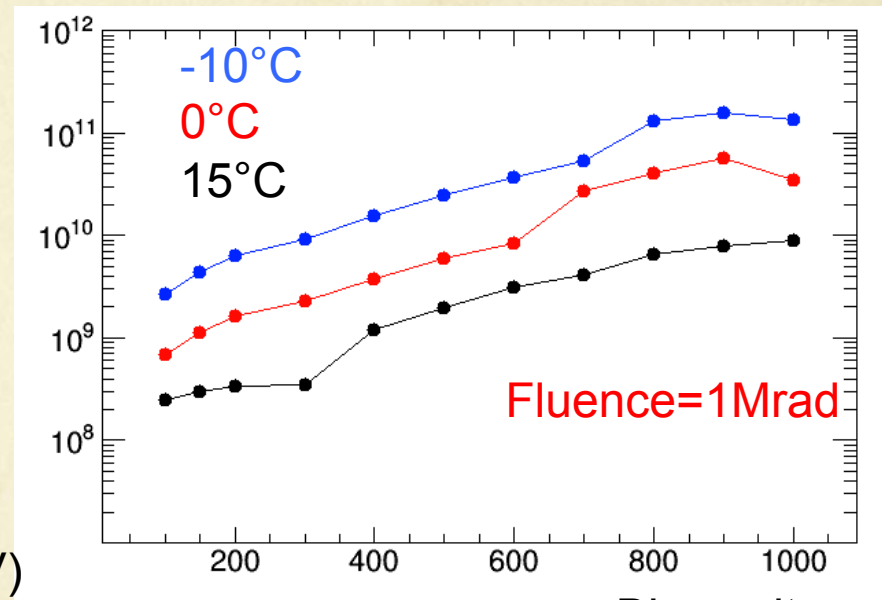
R\_INT( $\Omega/\text{cm}$ )



Bias voltage (V)

Biased voltage=-1000V

R\_INT( $\Omega/\text{cm}$ )



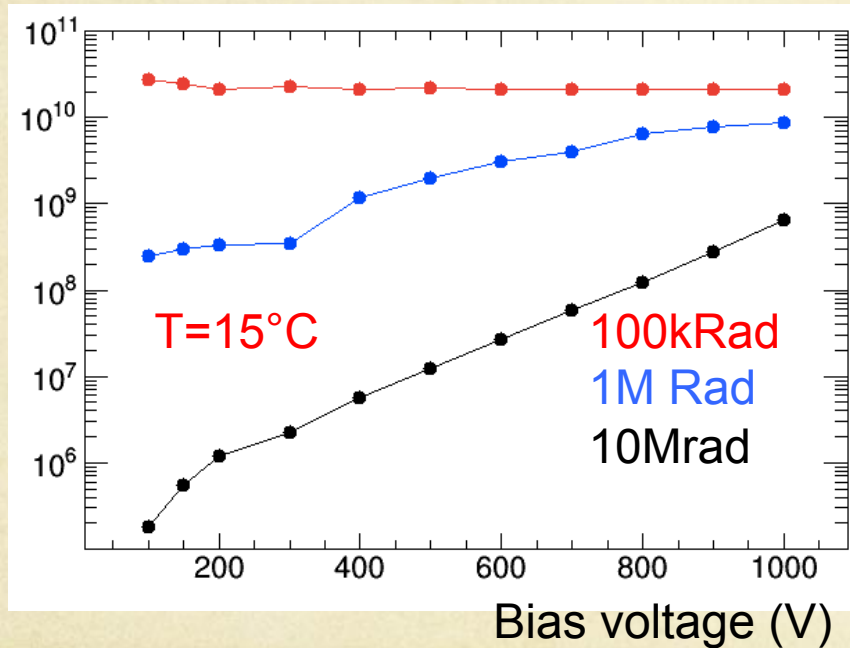
Bias voltage (V)

Fluence	$-10^\circ\text{C}$	$0^\circ\text{C}$	$15^\circ\text{C}$
10 Mrad	62.6 G $\Omega/\text{cm}$	5.3G $\Omega/\text{cm}$	0.64G $\Omega/\text{cm}$
1 MRad	136.5G $\Omega/\text{cm}$	35.0G $\Omega/\text{cm}$	8.8 G $\Omega/\text{cm}$

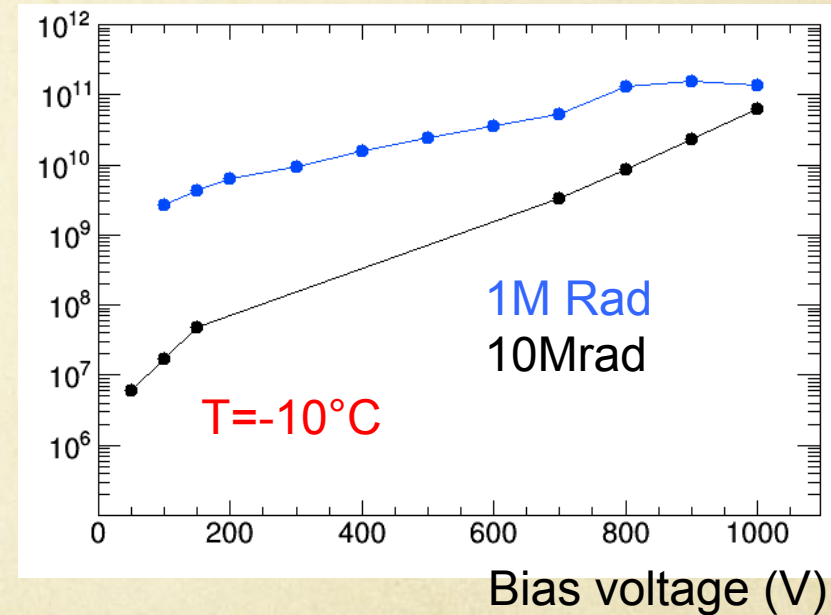
# Inter-strip resistance Vs bias voltage

- Higher bias voltage dependence as fluence increases

$R_{INT}(\Omega/cm)$



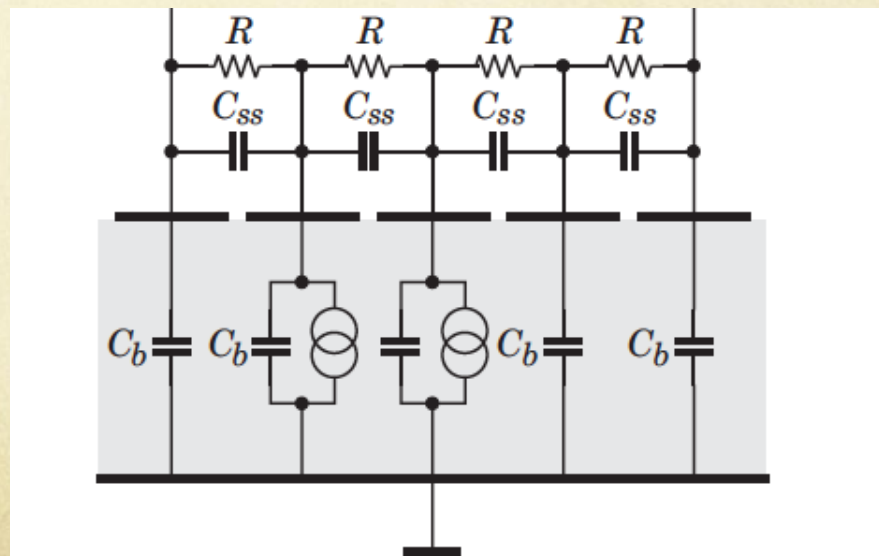
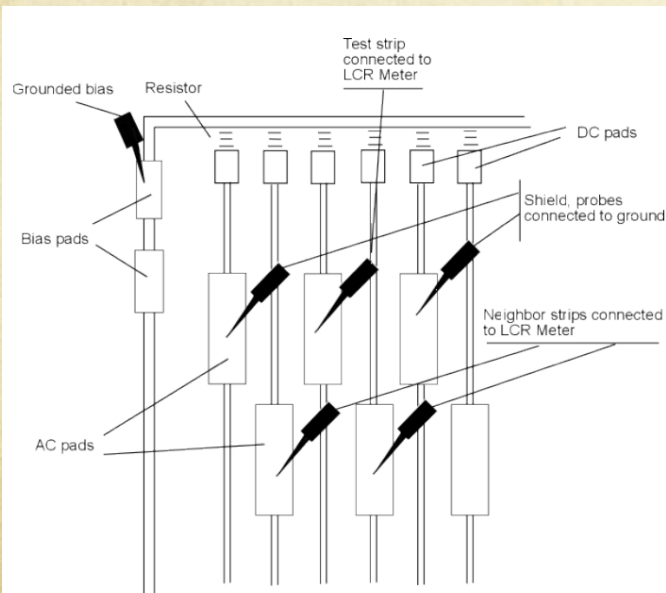
$R_{INT}(\Omega/cm)$





# Inter-strip capacitance

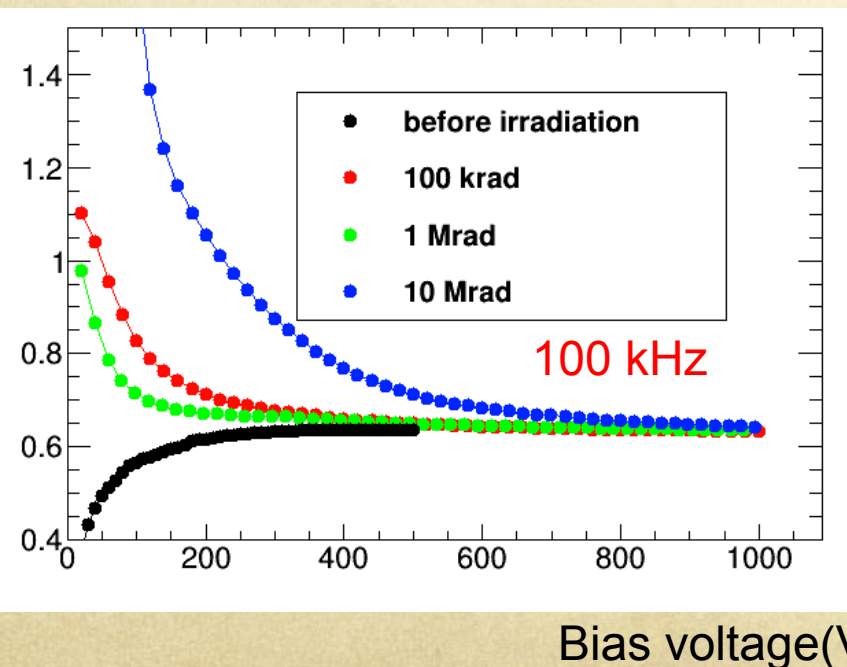
- ❑ Inter-strip resistance is the capacitance between strips
- ❑ Large Inter-strip resistance will cause higher cross talk noise
  - ❑ Reducing the signal to noise ratio
- 5 probe methods:
  - Middle strip connected to LCR meters low side
  - First neighbor strips connected to LCR meters high side.
  - The Second neighbor strips grounded



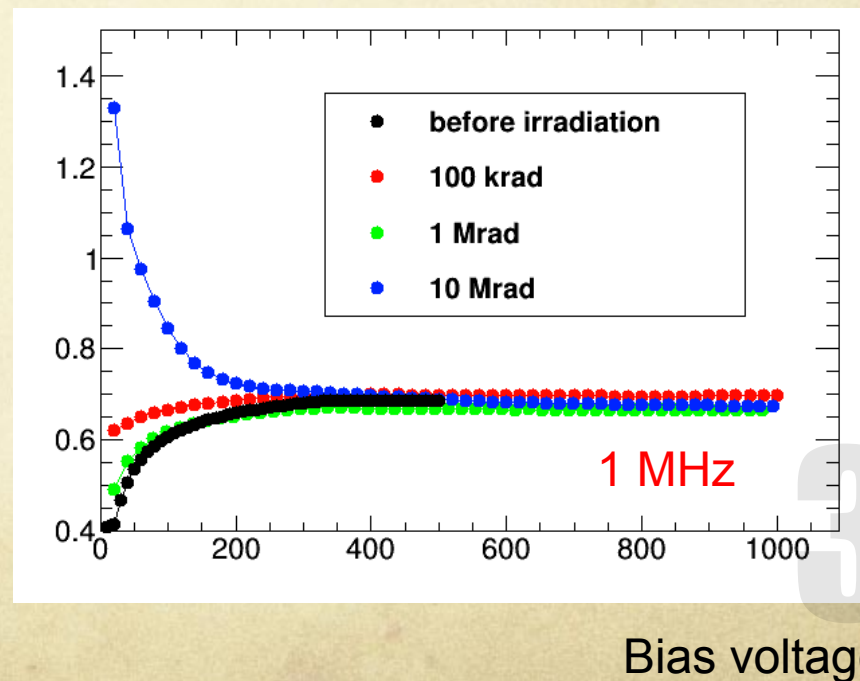
# Bias Voltage dependence

- Inter-strip capacitance shows a stronger bias voltage dependence at low frequency (i.e. 100kHz)

Inter-strip capacitance ( pF/cm)



Inter-strip capacitance ( pF/cm)



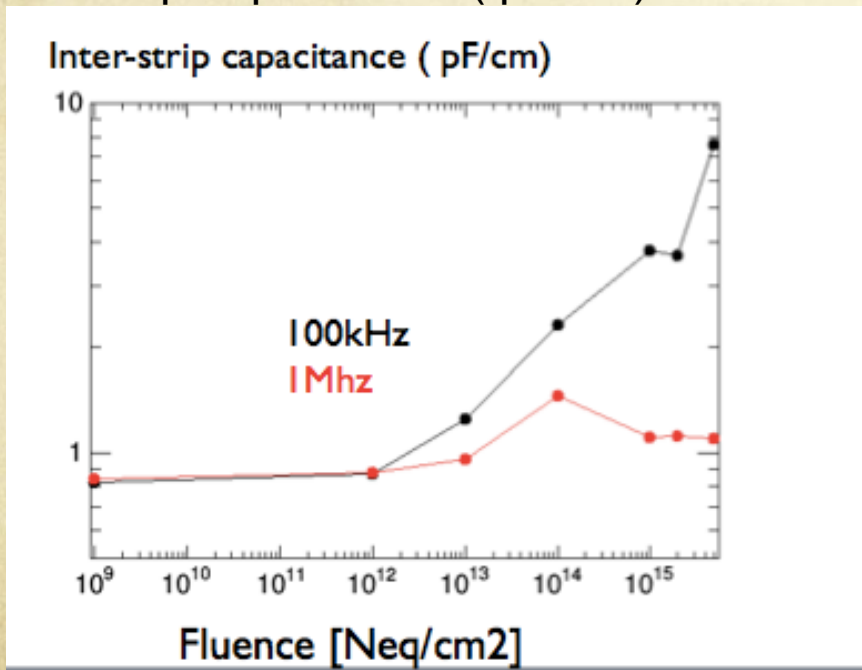


# Inter-strip capacitance VS Fluence

- Main result: Less impact by radiation in high frequency region
  - $C_{int}$  increase after radiation for slow signal (100Hz)
  - Have less impact for fast signal (MHz)

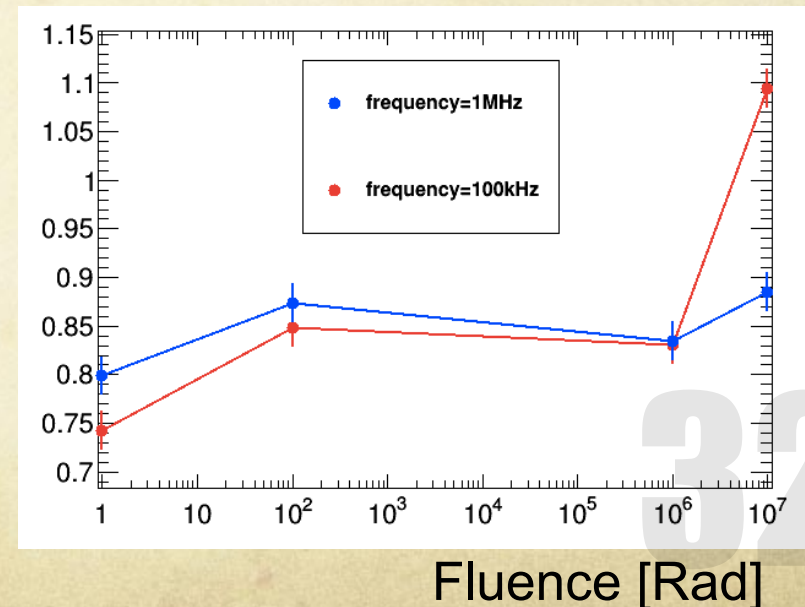
## Proton radiation

Inter-strip capacitance ( pF/cm)



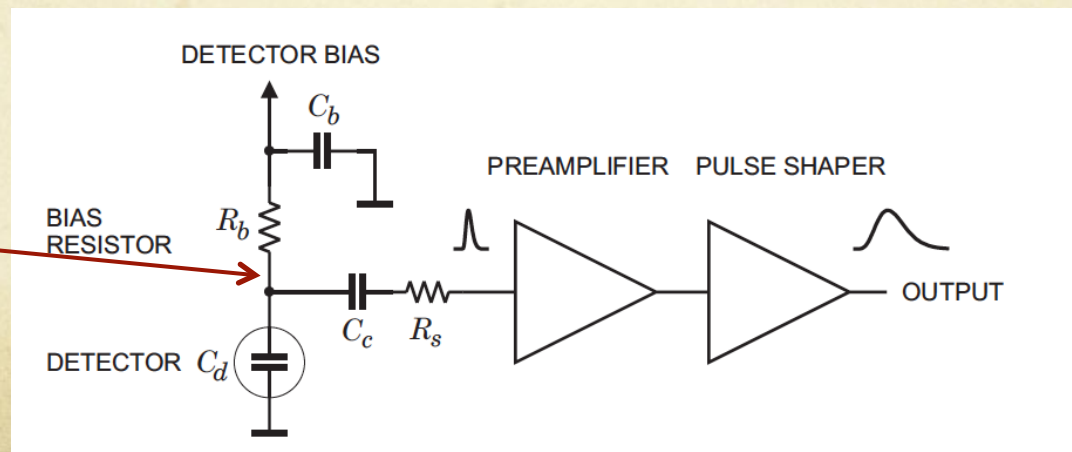
## Gamma radiation

Inter-strip capacitance ( pF/cm)



# Punch through protection design in planar sensor

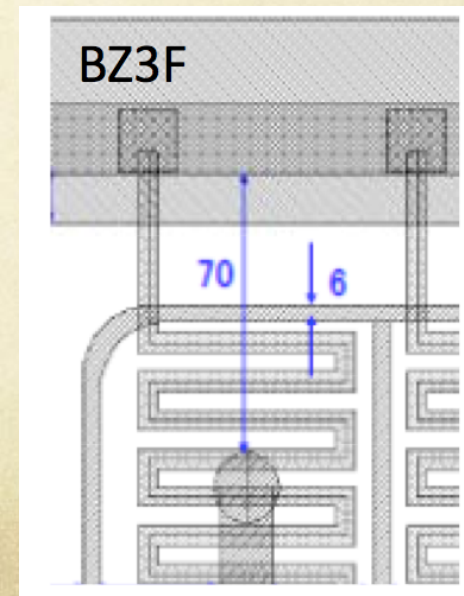
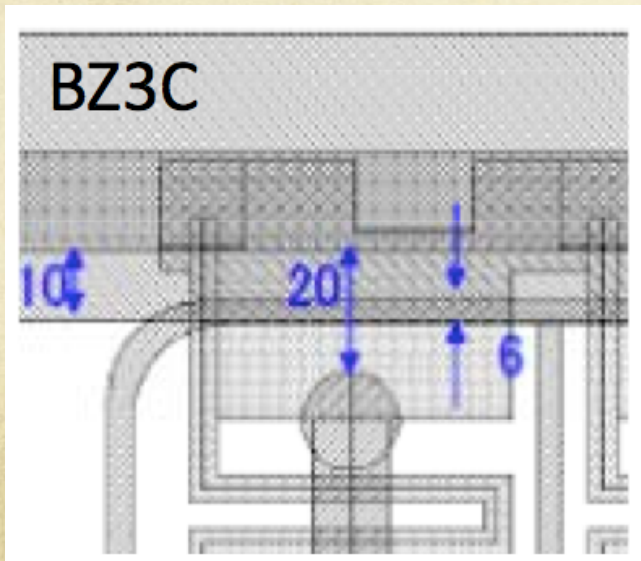
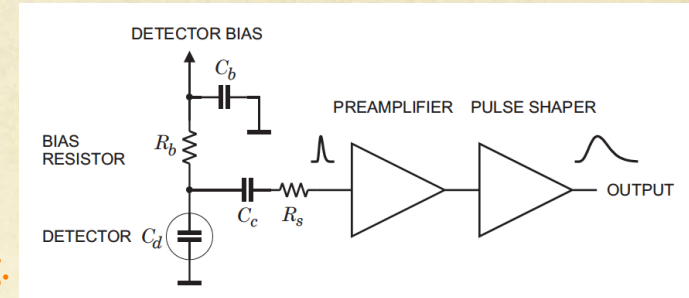
- When the proton beam is not stable or during beam loss
  - Lots of charge particle go through the sensors
- Large amount of charge accumulated before coupling capacitance
  - This accumulated is AC signal , can go through coupling capacitance
  - Large amount of signal will damage pre-amplifier





# Punch through protection design in planar sensor

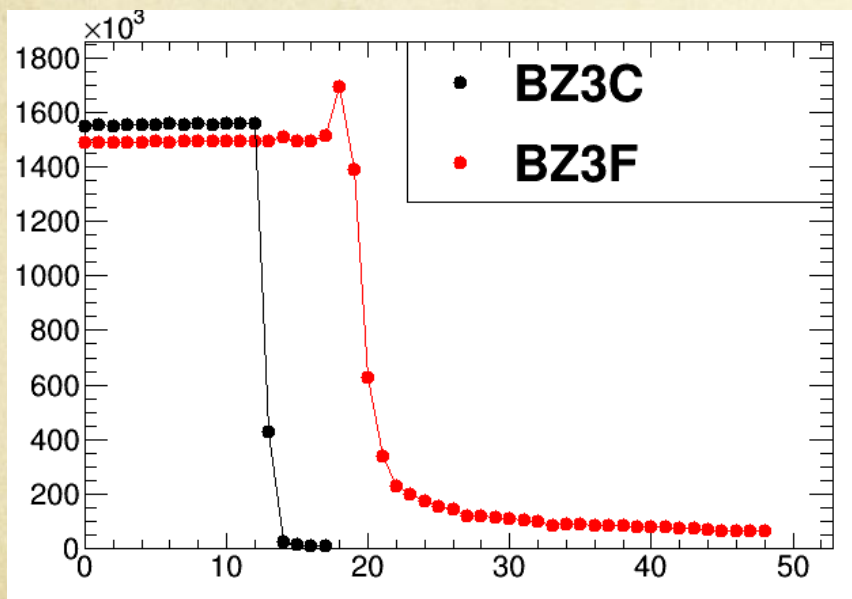
- Design punch through protection
  - P-n-p transistor structure
  - Two design:
    - Varying the distance between p stop and bias ring.
- The  $R_b$  is short when accumulated charge is large



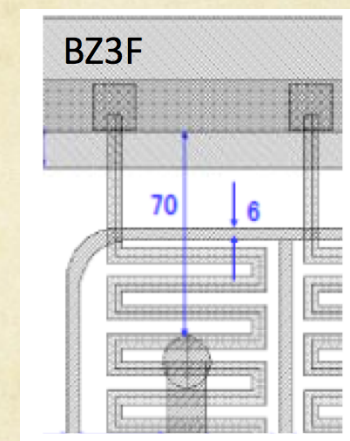
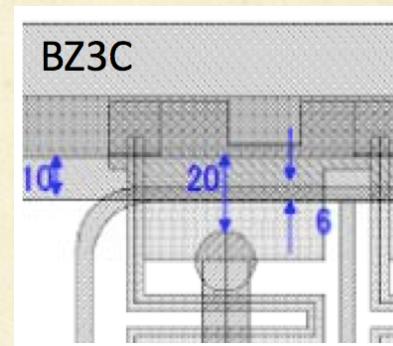
# Punch through protection performance

- BZ3C has a smaller punch-through voltage before radiation.
- After radiation, both sensors have similar punch-through voltage
- PTP structure is still working well in BZ3C

Resistance(Ohm)



Voltage (V)





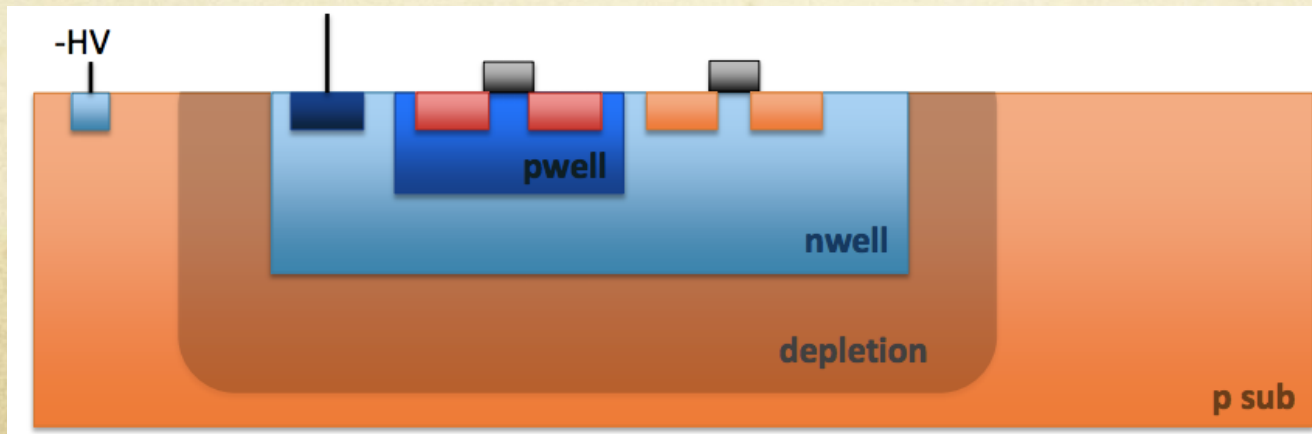
# Introduction to CMOS sensor for strip detector application

- ATLAS ITK silicon strip detector phase 2 upgrade
- Sensor status
  - Default solution : n-on-p type planar sensors
  - Alternative solution : CMOS pixel sensors



# CMOS pixel sensors developments

- Implemented in commercial CMOS (HV) technologies (350nm, 180nm)
  - Collection electrode is a large n-well/p-substrate diode
- Advantage:
  - High granularity: pitch can be reduced to below 50 $\mu$ m
  - low material budget : Can be thinned down to 50 $\mu$ m
  - Monolithic: Front-end electronics and sensor can be built in the same chip
  - Low cost
- Drawback:
  - Low MIP signal : 1000~2000 e



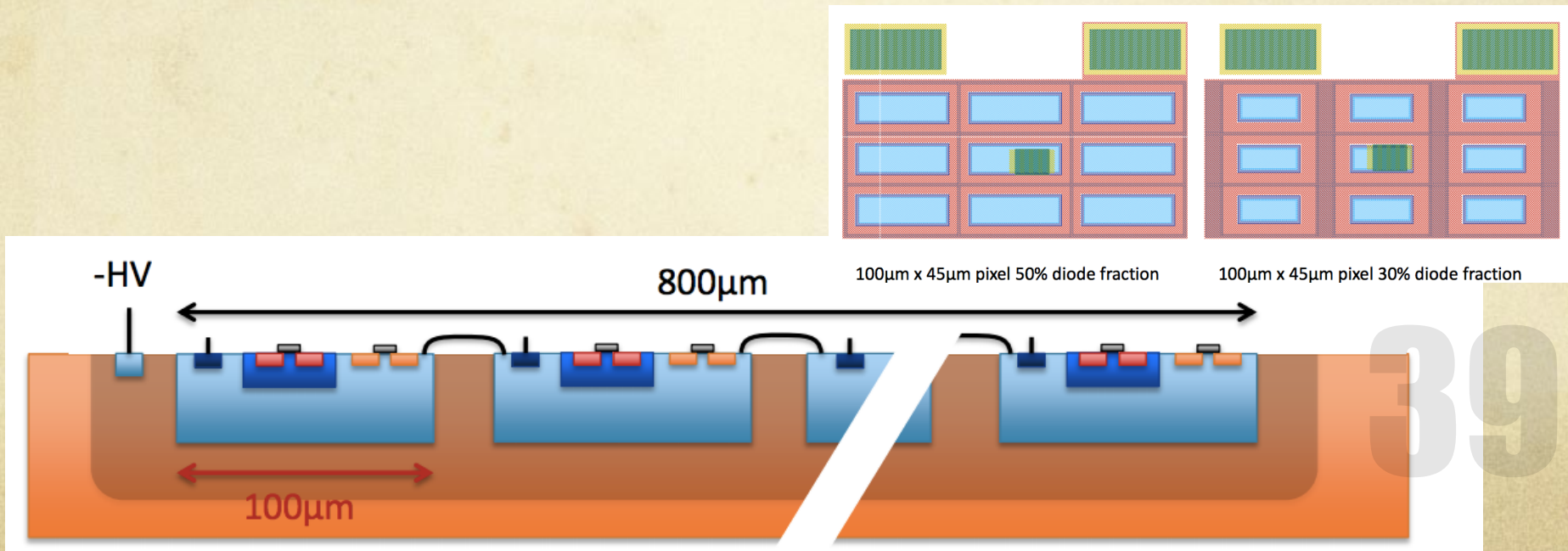
# CMOS pixel sensors in ATLAS

- ATLAS agreed to explore the possible use of the technology, with 3-year plan:
- Year 1: Characterization of basic sensor/electronics properties and architecture
- Year 2: Fabricating and evaluating a large-scale device.
- Year 3: Full prototypes of sensors and ABCN' readout chip



# HV-CMOS pixel array design

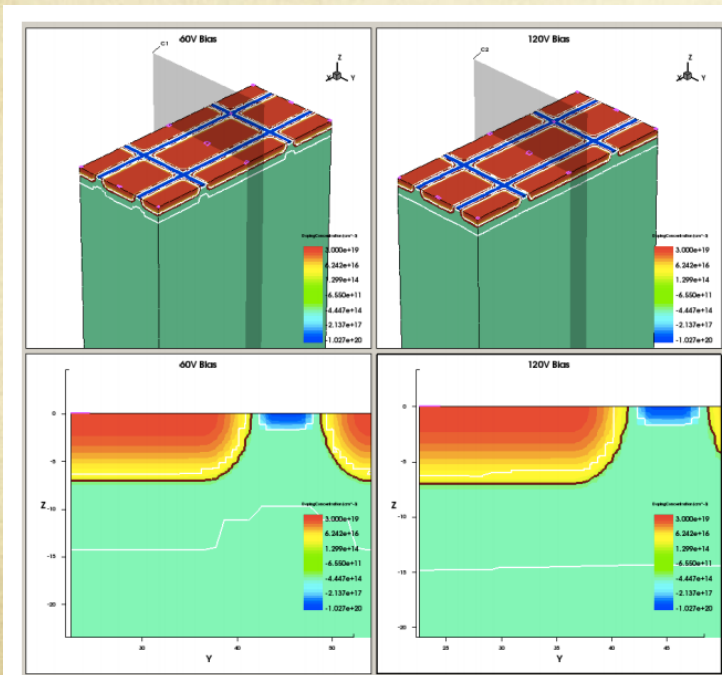
- For strip application, larger pixel size is considered in the last submission
  - $45\mu\text{m} \times 100\mu\text{m}$  ,  $45\mu\text{m} \times 200\mu\text{m}$ ,  $45\mu\text{m} \times 400\mu\text{m}$   $45\mu\text{m} \times 800\mu\text{m}$
  - 30%-50% Nwell fraction
    - Expect better performance in higher Nwell fraction
  - Electronics in the strip allow for strip segmentation
  - – AMS provides options for high resistivity substrate
    - Substrate resistivity can be up to a few thousand  $\Omega$



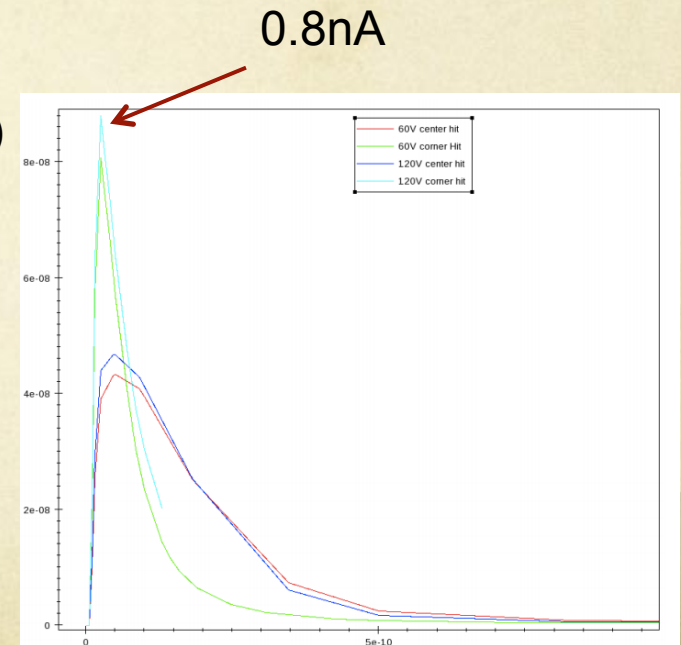


# HV-CMOS pixel array design

- Other designed proprieties in simulation
  - Depletion region
  - Nwell capacitance
  - Charge collected
- Drift time is designed to be 0.1-0.5ns
- low signal amplitude
  - Can not be readout directly, need amplifier



Current (A)



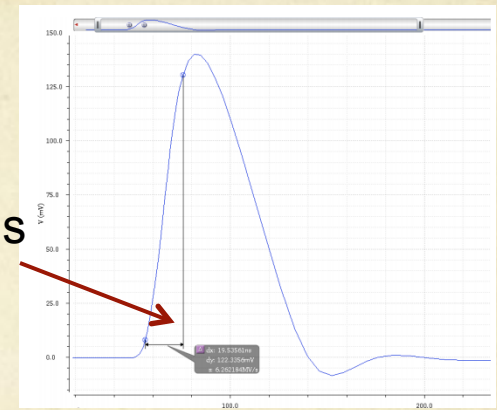
Simulation results from SLAC

Time (s)

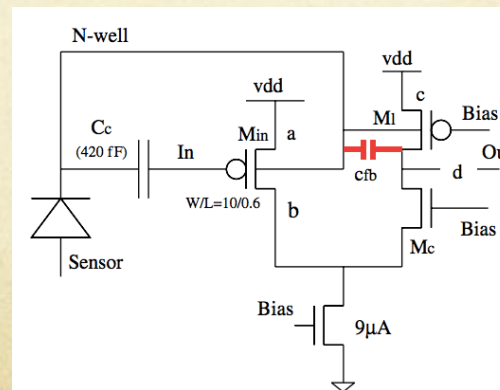
# Design of amplifier

- signal to noise ratio is relatively low in HV-CMOS sensors
  - A monolithic design of a built-in low-noise amplifier is needed
    - The pixel array and amplifier are designed in the same chip
    - The noise of the monolithic amplifier is designed to be lower than external amplifier
  - The amplifier design must be radiation hard
    - radiation tolerant layout techniques is used
  - The raise time should be fast as well for LHC application
    - 16ns raise time for active pixel signal after amplification

16ns



Time (s)

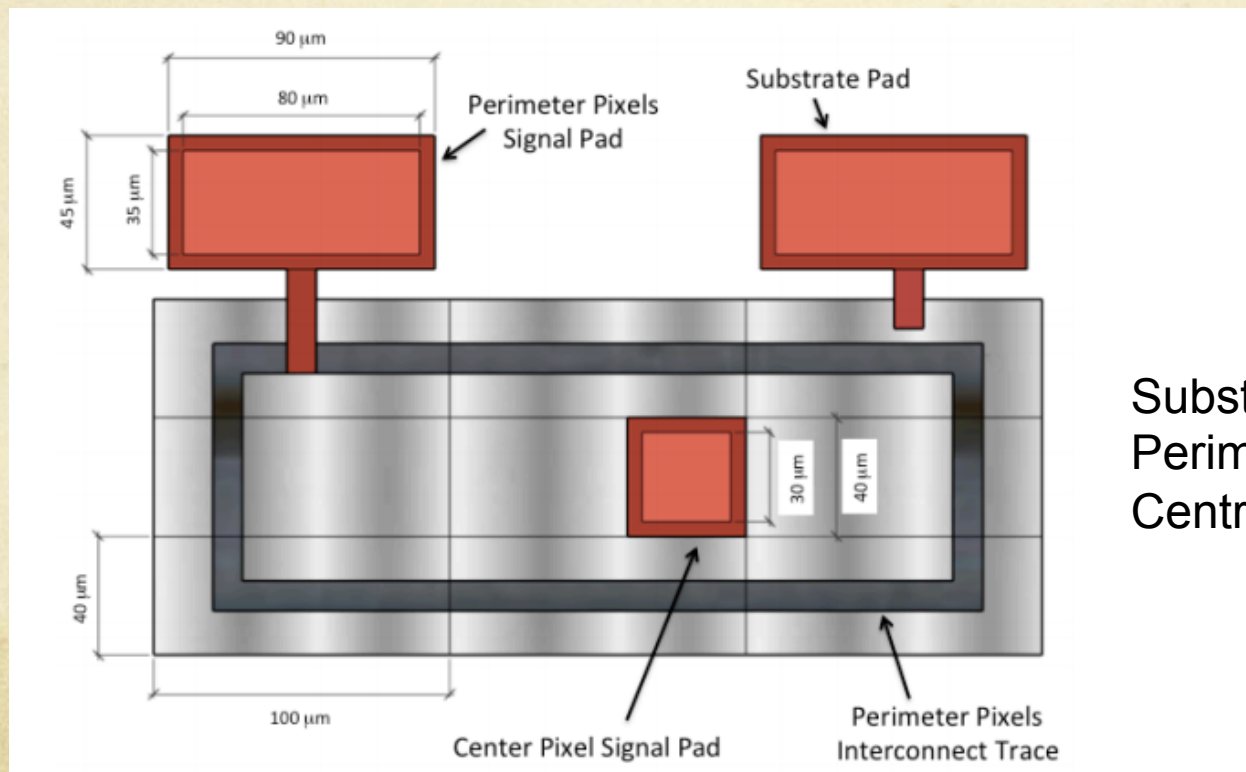


Specifications	Simulated values
Rise time	16 ns (10 - 90 %)
Noise	200 e <sup>-</sup>
Gain	500 mV/fC
Power consumption	210μW/ amplifier
Pulse duration	50ns

Designed by UC Santa Cruz

# Testing setup and major Challenge

- Compared to conventional planar sensors for strip detector
  - Leakage current in single pixel is about much lower by five order of magnitude
  - Capacitance is lower by at least 10 times compared to single strip in planar sense
  - Need setup for low noise measurement

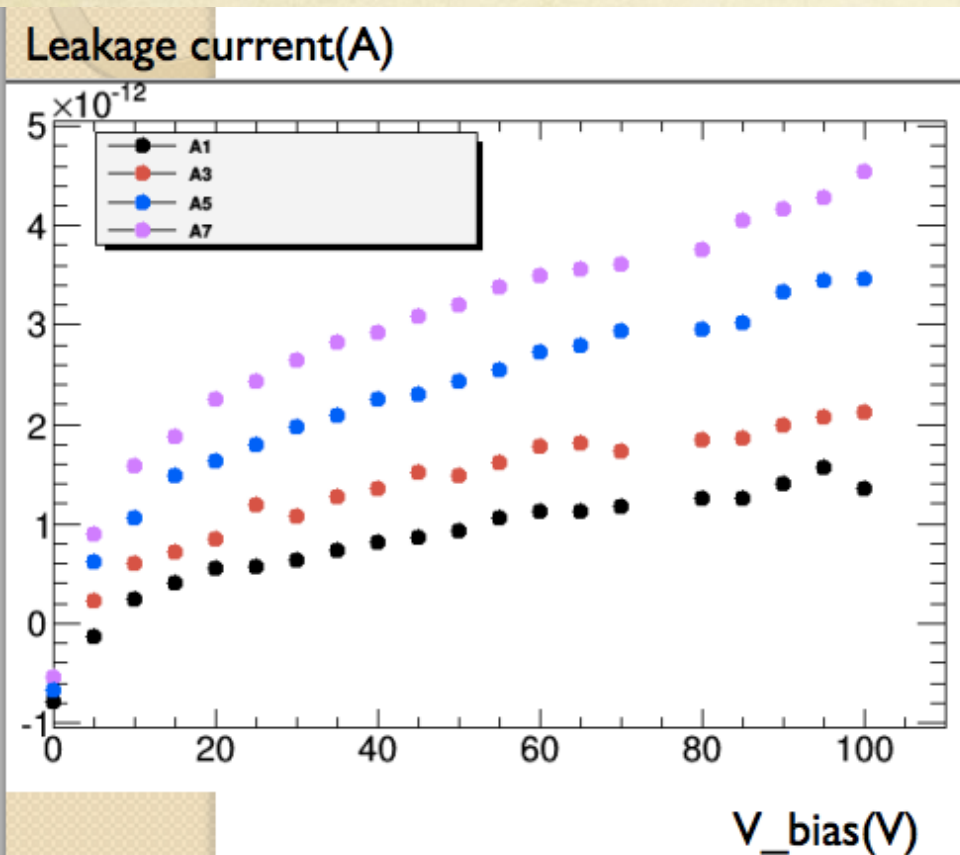


Substrate: grounded  
Perimeter pixels: +HV  
Central pixel: +HV



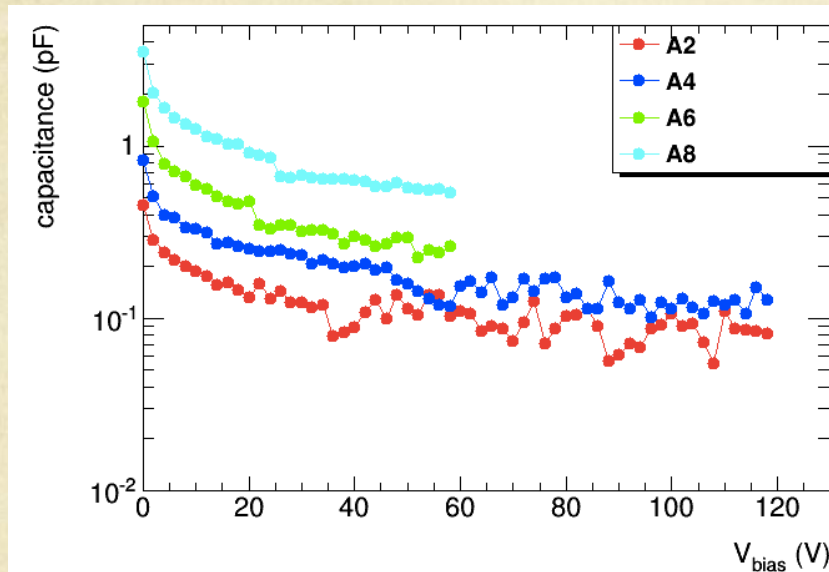
# Central pixel IV

- I-V measurement
  - Can Biased up to 120V without breakdown
  - Low leakage current (pA level)
  - Leakage current proportional to pixel size.



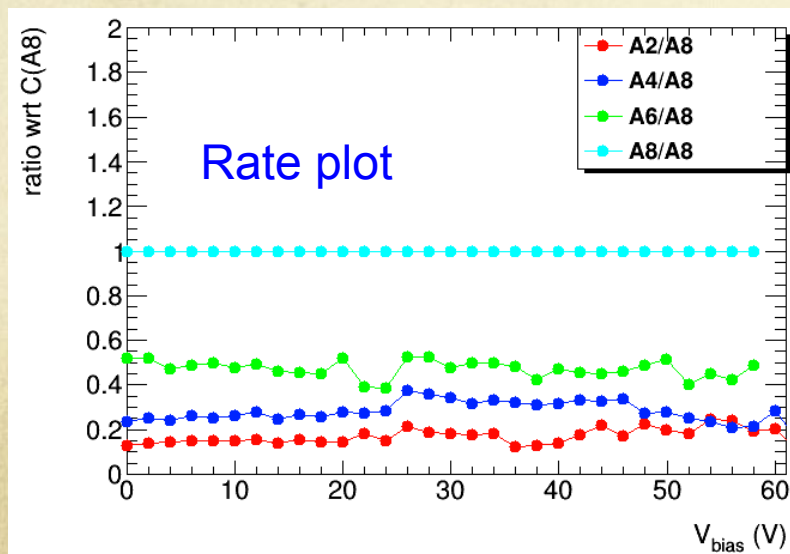
PPA #	Pixel width	Pixel length	Diode Area Fraction	Metal opening ratio
PPA01	45 $\mu m$	100 $\mu m$	30%	13.0%
PPA03	45 $\mu m$	200 $\mu m$	30%	22.7%
PPA05	45 $\mu m$	400 $\mu m$	30%	27.4%
PPA07	45 $\mu m$	800 $\mu m$	30%	29.8%

# Capacitance of central pixel array with different size



The central pixel capacitance at low bias voltage is roughly proportional to pixel size.

- ☐ At low bias voltage
- ☐  $C(A4)$  is about  $1/2$  of  $C(A8)$
- ☐  $C(A6)$  is about  $1/4$  of  $C(A8)$
- ☐  $C(A2)$  is about  $1/8$  of  $C(A8)$

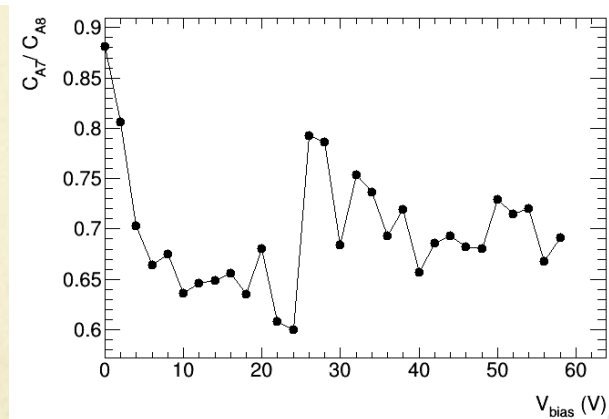
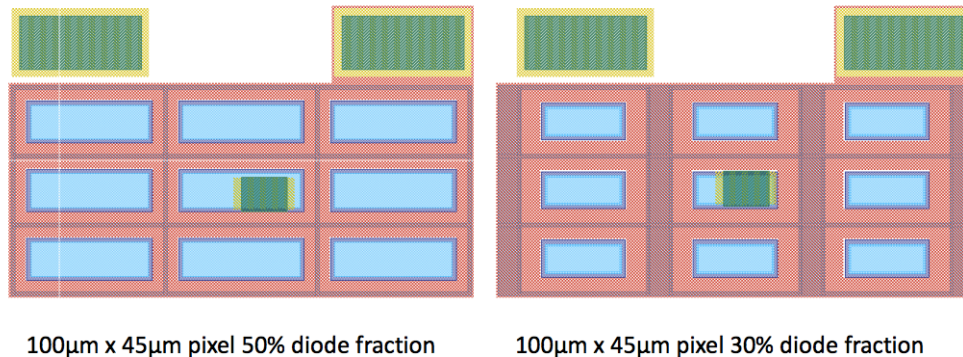
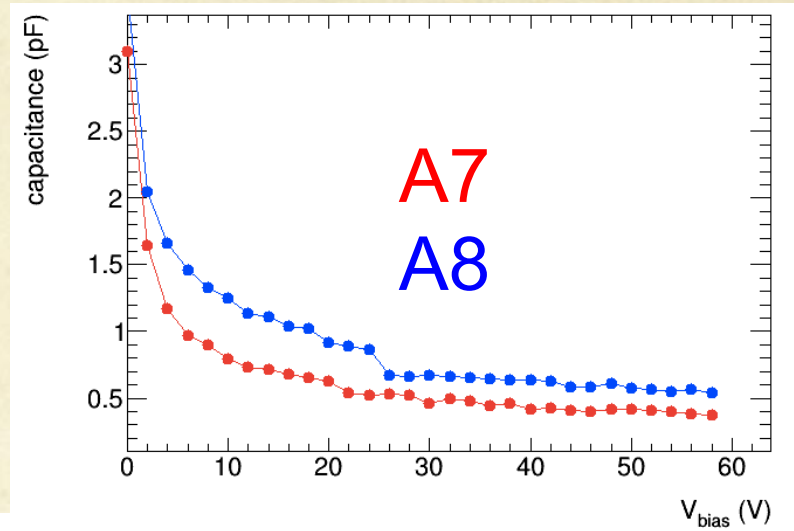


PPA #	Pixel width	Pixel length	Diode Area Fraction	Metal opening ratio
PPA02	45 $\mu$ m	100 $\mu$ m	50.4%	34.5%
PPA04	45 $\mu$ m	200 $\mu$ m	50.4%	44.0%
PPA06	45 $\mu$ m	400 $\mu$ m	50.4%	48.7%
PPA08	45 $\mu$ m	800 $\mu$ m	50.4%	51.0%

# Capacitance of pixel array with different diode area fraction

PPA #	Pixel width	Pixel length	Diode Area Fraction	Metal opening ratio
PPA07	45 $\mu\text{m}$	800 $\mu\text{m}$	30%	29.8%
PPA08	45 $\mu\text{m}$	800 $\mu\text{m}$	50.4%	51.0%

Observe lower capacitance for pixel with lower diode fraction



□  $C(A7)$  is about 70% of  $C(A8)$

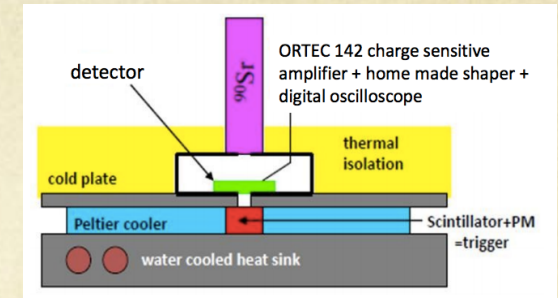


# Charge collection measurements

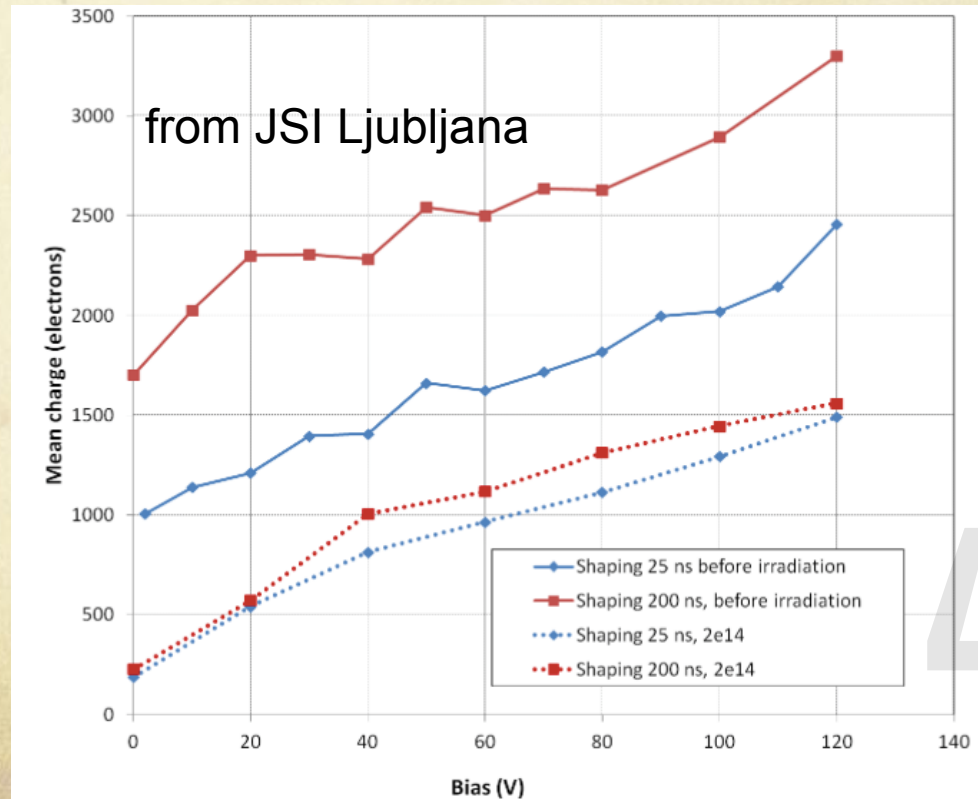
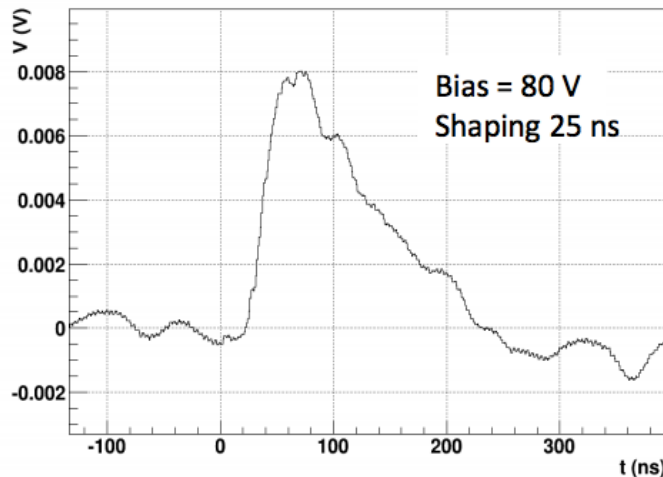
from JSI Ljubljana

Use CMOS pixel for charge collections tests

- Signal to noise ratio is about 10 using external amplifier
- 60% charge efficiency after  $2 \times 10^{14}$  Neq/cm<sup>2</sup> proton radiation



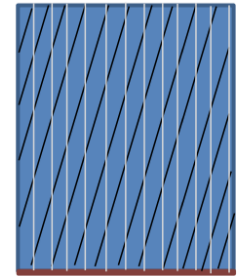
from JSI Ljubljana



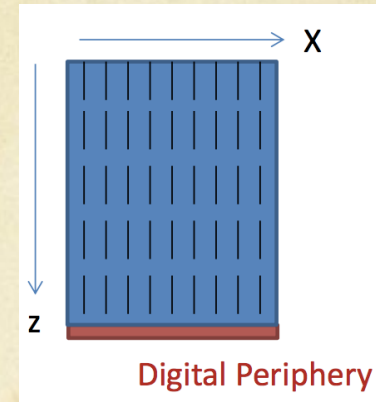
46

# Architectures design

Built-in Stereo- Two set of connections on pixel matrix



CMOS Periphery



Digital Periphery

- Two designs are considered
- Built-in Stereo:
  - Readout binary in two set of connections on pixel matrix
  - similar to conventional planar sensor
  - not able to use the advantage of CMOS technology
- Digital Z encode: (to be test in March 2015 submission)
  - Z encoding is found to be the best design
  - Not a binary readout, readout the address of the hits
  - In the example segment : 40X800um
    - readout 9 bits of 'x; position
    - readout 5 bits of 'z' position
    - Only needed 14 wire bond in this example
      - Reduce the number of wire bonding by order of magnitude
    - Save a lot of module building time
- Amplification and digitization will be done in HV-CMOS chip



# Short summary of CMOS sensor testing

- Preliminary I-V and capacitance results for HV-CMOS CHESSI chips
  - **I-V measurement**
    - Can Biased up to 120V without breakdown
    - Low leakage current (pA level)
  - **C-V measurement**
    - The central pixel capacitance at low bias voltage is roughly proportional to pixel size.
    - Observe lower capacitance for pixel with lower diode fraction
  - **Charge collections efficiency**
    - Signal to noise ratio is about 10
    - 60% charge efficiency after  $2 \times 10^{14}$  Neq/cm<sup>2</sup> proton radiation
    -



# Next step for CMOS sensor development

- Sensor testing
  - Testing the performance of the built-in amplifier
  - Measure I-V curve and capacitance of the CMOS pixel after radiation
  - Study charge collection efficiency after radiation
- Next big milestone :
  - Next submission in March 2015 is planned to test digitation and Digital Z encoding readout

# Summary

- Motivation of ATLAS upgrade
  - Physics case in gauge boson self coupling
  - Physics case in VBF  $H(bb)+\gamma$ 
    - for  $H \rightarrow bb$  coupling and VBF Higgs production mechanism study
- Radiation hardness study for conventional strip sensor for ATLAS strip detector upgrade
- CMOS pixel as alternative sensor solution in ATLAS strip detector application



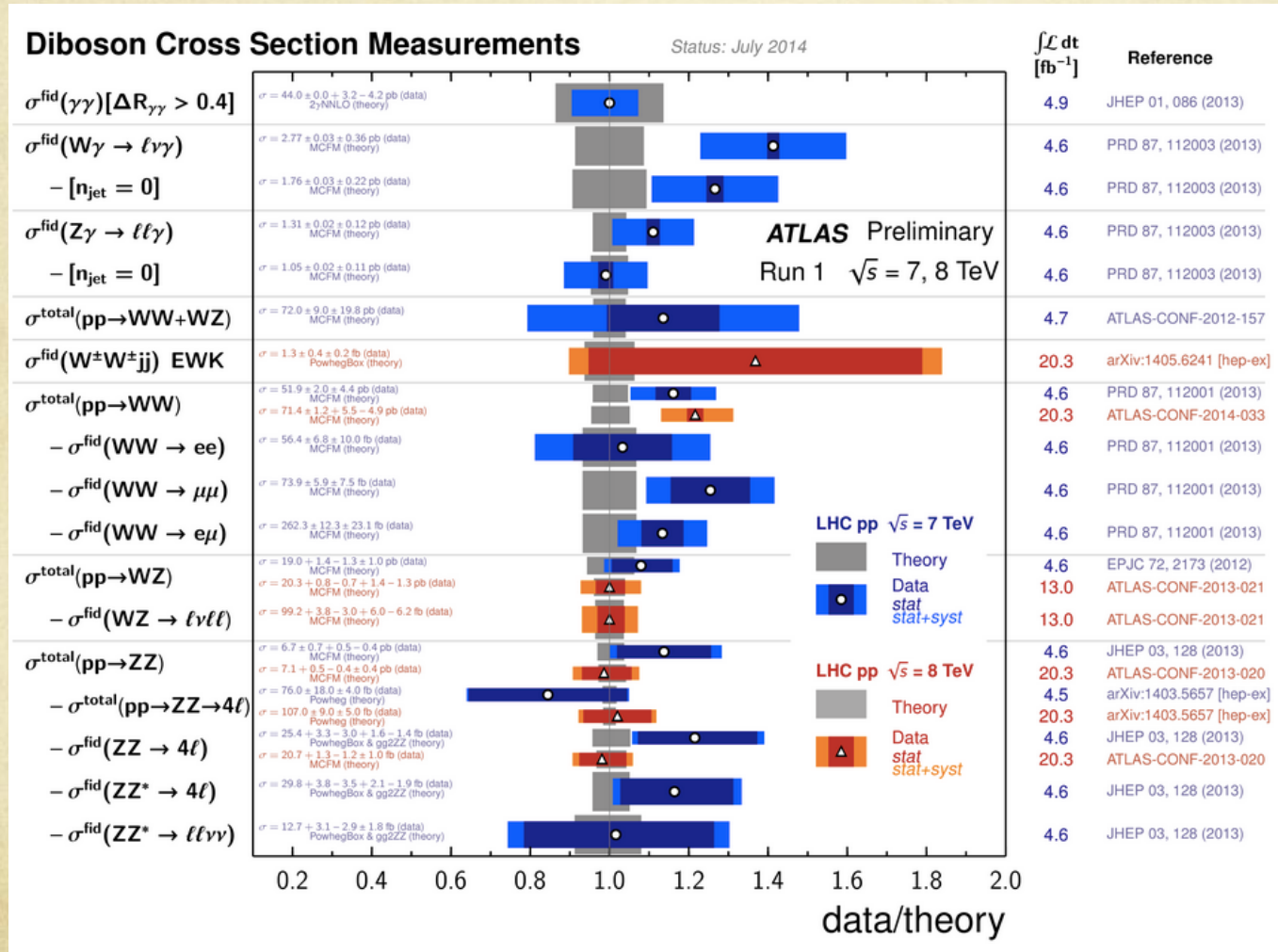
backup



# Diboson cross sections measurements overview

## Cross-section measurements

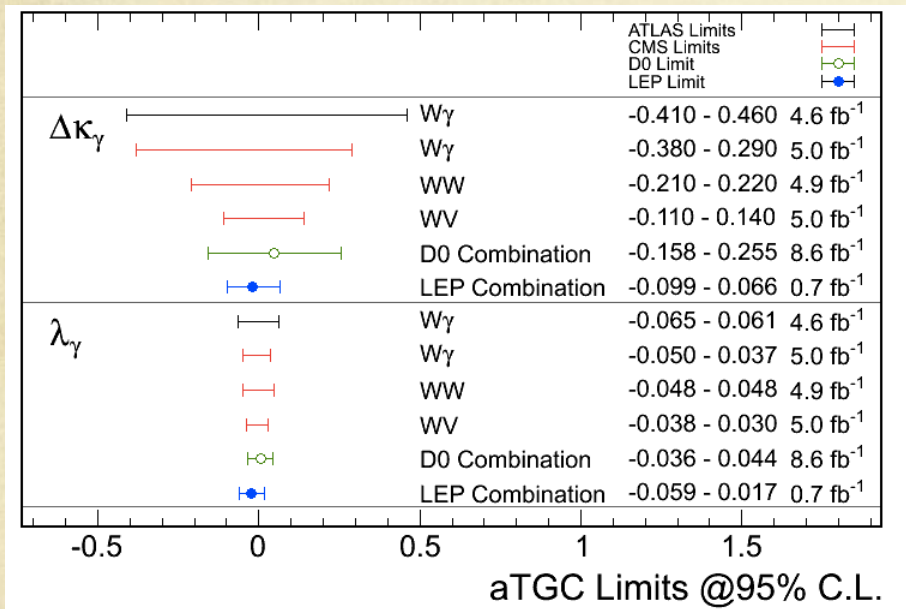
- performed in  $WW, ZZ, WZ, W\gamma$  and  $Z\gamma$  channels
- Latest 8TeV results Improved accuracy compared to 7TeV



# Triple Gauge Couplings

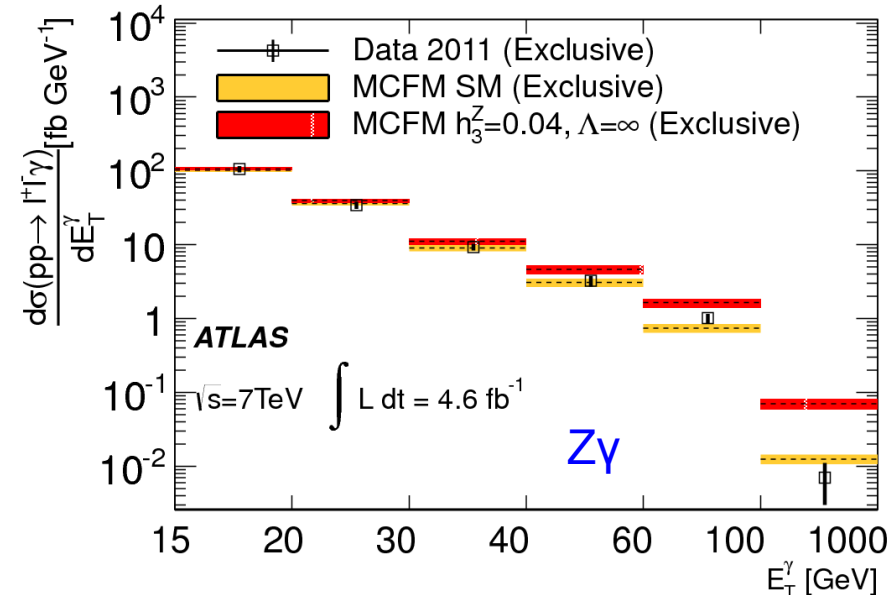
- The s-channel diagrams contain the triple gauge coupling vertex
- New physics may modify these couplings.
- aTGCs modify the event kinematics
  - Effects of aTGCs increase with  $s^{\wedge}$

coupling	parameters	channel
$WW\gamma$	$\lambda_{\gamma}, \Delta\kappa_{\gamma}$	$WW, W\gamma$
$WWZ$	$\lambda_Z, \Delta\kappa_Z, \Delta g_1^Z$	$WW, WZ$
$ZZ\gamma$	$h_3^Z, h_4^Z$	$Z\gamma$
$Z\gamma\gamma$	$h_3^{\gamma}, h_4^{\gamma}$	$Z\gamma$
$Z\gamma Z$	$f_{40}^Z, f_{50}^Z$	$ZZ$
$ZZZ$	$f_{40}^{\gamma}, f_{50}^{\gamma}$	$ZZ$



Charged aTGCs

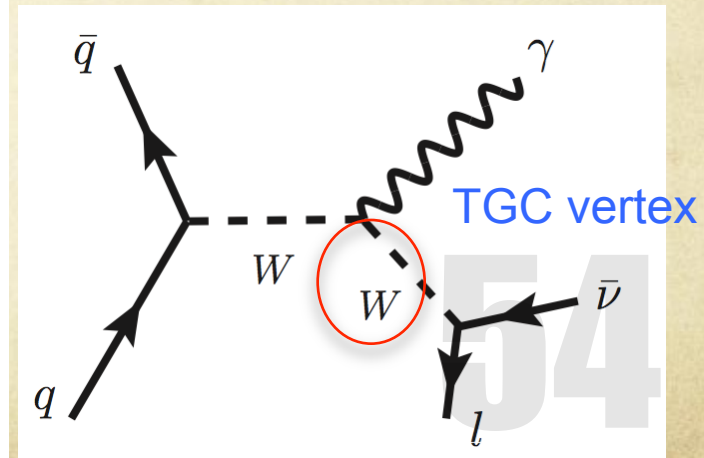
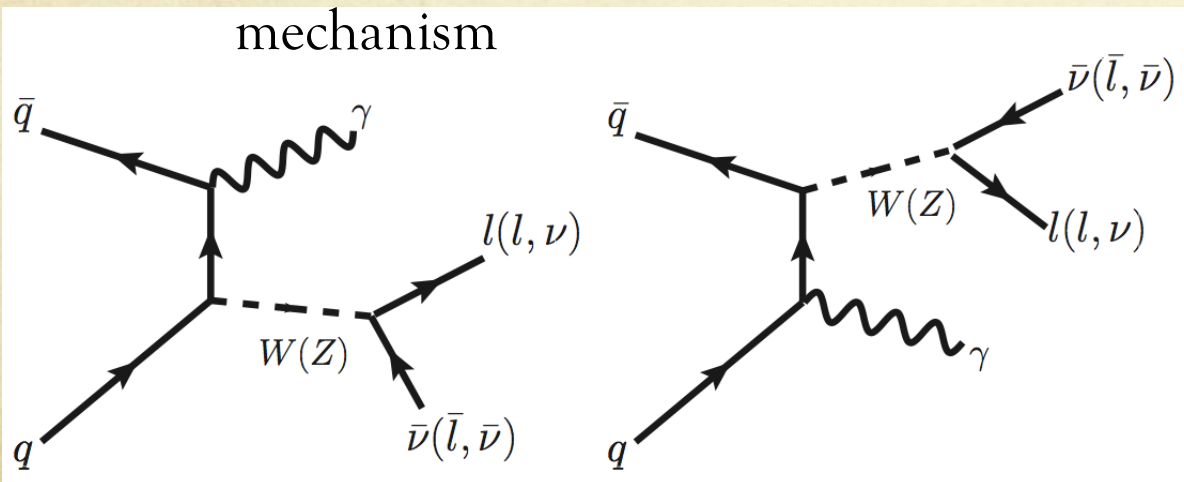
aTGC limits is comparable or better than Tevatron results





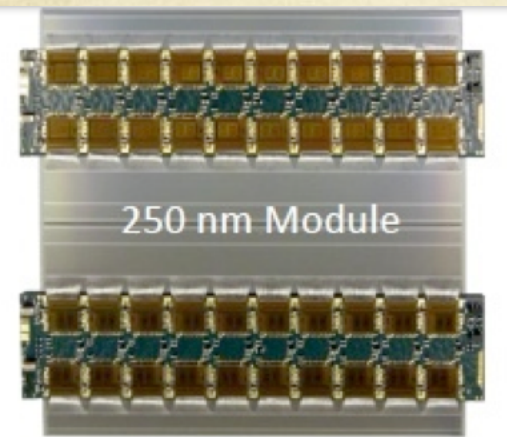
# Motivation of diboson physics

- Diboson production cross-section measurements
  - Test of SM electroweak theory and perturbative QCD at TeV scale
  - Sensitivity to new particles decaying to dibosons (Technicolor, Little Higgs, SUSY, etc...)
- Anomalous Triple Gauge Couplings (aTGC)
  - The Higgs mechanism  $\neq$  a Higgs boson !
  - Vector boson self-couplings fundamental prediction of the Electroweak Sector of SM
  - Its study is important to understanding electroweak symmetry mechanism



# Stave design in strip detector

- **Hybrid** = kapton board with FE chips (ABCNext, connection via wire bonds)
- **Module** = silicon sensor with readout hybrid (connection via wire bonds)
- **stave** = core structure + cooling + electrical services (power, data, TTC) + modules



This “module” is directly glued on top of the kapton bus tape

